


## Article

# Influence of Land Use and Topographic Factors on Soil Organic Carbon Stocks and Their Spatial and Vertical Distribution

Kyle W. Blackburn<sup>1</sup>, Zamir Libohova<sup>2,\*</sup>, Kabindra Adhikari<sup>3</sup> , Charles Kome<sup>4</sup>, Xander Maness<sup>1</sup> and Miles R. Silman<sup>1,5</sup>

- <sup>1</sup> Department of Biology, Wake Forest University, Winston-Salem, NC 27109, USA; blackw17@alumni.wfu.edu (K.W.B.); xander\_maness@alumni.wfu.edu (X.M.); silmanmr@wfu.edu (M.R.S.)
- <sup>2</sup> Dale Bumpers Small Farms Research Center, Agricultural Research Service, United States Department of Agriculture, Booneville, AK 72927, USA
- <sup>3</sup> Grassland, Soil & Water Research Laboratory, Agricultural Research Service, United States Department of Agriculture, Temple, TX 76502, USA; kabindra.adhikari@usda.gov
- <sup>4</sup> Natural Resources Conservation Service, United States Department of Agriculture, Washington, DC 20540, USA; charles.kome@usda.gov
- <sup>5</sup> Center for Energy, Environment, and Sustainability, Wake Forest University, Winston-Salem, NC 27109, USA
- \* Correspondence: zamir.libohova@usda.gov; Tel.: +1-(402)-318-1146

**Abstract:** Soil organic carbon (SOC) plays a critical role in major ecosystem processes, agriculture, and climate mitigation. Accurate SOC predictions are challenging due to natural variation, as well as variation in data sources, sampling design, and modeling approaches. The goal of this study was to (i) understand SOC stock distribution due to land use (restored prairie grass—PG; lawn grass—LG; and forest—F), and local topography, and (ii) assess the scalability of SOC stock predictions from the study site in North Carolina (Lat: 36°7' N; Longitude: 80°16' W) to the geographic extension of the Fairview soil series based on the US Soil Survey Geographic (gSSURGO) database. Overall, LG had the highest SOC stock (82 Mg ha<sup>−1</sup>) followed by PG (79 Mg ha<sup>−1</sup>) and forest (73.1 Mg ha<sup>−1</sup>). SOC stock decreased with the depth for LG and PG, which had about 60% concentrated on the surface horizon (0–23 cm), while forest had only 40%. The differences between measured SOC stocks and those estimated by gSSURGO and modeled based on land use for the Fairview series extent were comparable. However, subtracting maps of the uncertainty predictions based on the 90% confidence interval (CI) derived from the measured values and estimated gSSURGO upper and lower values (an estimated CI) resulted in a range from −17 to 41 Mg ha<sup>−1</sup> which, when valued monetarily, varied from USD 33 million to USD 824 million for the Fairview soil series extent. In addition, the spatial differences found by subtracting the gSSURGO estimations from measured uncertainties aligned with the county administrative boundaries. The distribution of SOC stock was found to be related to land use, topography, and soil depth, while accuracy predictions were also influenced by data source.

**Keywords:** soil organic carbon prediction; soil horizons; LiDAR; extrapolation uncertainty; regression kriging



**Citation:** Blackburn, K.W.; Libohova, Z.; Adhikari, K.; Kome, C.; Maness, X.; Silman, M.R. Influence of Land Use and Topographic Factors on Soil Organic Carbon Stocks and Their Spatial and Vertical Distribution. *Remote Sens.* **2022**, *14*, 2846. <https://doi.org/10.3390/rs14122846>

Academic Editor: Maruthi Sridhar Balaji Bhaskar

Received: 5 April 2022

Accepted: 6 June 2022

Published: 14 June 2022

**Publisher's Note:** MDPI stays neutral with regard to jurisdictional claims in published maps and institutional affiliations.



**Copyright:** © 2022 by the authors. Licensee MDPI, Basel, Switzerland. This article is an open access article distributed under the terms and conditions of the Creative Commons Attribution (CC BY) license (<https://creativecommons.org/licenses/by/4.0/>).

## 1. Introduction

Soil organic carbon (SOC) plays a critical role in several ecosystem processes that are important to agriculture. For example, SOC is (i) a medium for plant growth and food production [1]; (ii) maintains and stabilizes soil structure; and (iii) improves available water-holding capacity and water infiltration, in addition to reducing erosion [2–4]. SOC stocks are the largest terrestrial carbon pool [5,6], containing—to a depth of 2 m—five times as much carbon compared to atmospheric CO<sub>2</sub> and other terrestrial biota [7,8]. SOC management is thus a key opportunity to mitigate the effects of climate change [5–10]. The recent initiative to increase SOC stock annually by “4 per 1000” (0.4% year<sup>−1</sup>) highlights the critical role that SOC is expected to play in reducing atmospheric CO<sub>2</sub> [11,12]. In this

context, understanding the dynamics that control SOC stocks in soils is a step forward in achieving the goals of the 4 per 1000 initiative.

Many factors such as climate [13–17], land use and management [13,18], terrain characteristics [19–24] and their interactions influence SOC stock dynamics. Climatic factors such as temperature, precipitation, and resulting soil moisture control organic matter decomposition and oxidation in soil [13,25,26]. Changes in temperature and precipitation can make SOC vulnerable to changes over time [27]. Research has shown that soils in colder and wetter climate conditions tend to have, overall, as much as three times more SOC compared to warmer and drier climates [1].

Within climatic regions, anthropogenic factors such as land use and management can play an important role [28–30]. For example, while SOC stocks have been shown to be vulnerable to shifts in temperature and precipitation [27], improved soil management and increased soil resilience have been shown to alleviate projected losses of SOC [31]. On the other hand, changes in land use practices have been shown to have a significant impact on SOC [13,18] and on soil depth as well [32–34]. Depending on the type of land use changes, SOC stocks can decrease [35] or increase [36,37]. In many instances, for areas heavily managed by humans, anthropogenic drivers can dominate SOC stock dynamics over natural drivers [30,38–41], especially land use changes and vegetation types [18,35–37].

The interaction of climate and land use are best observed at a landscape scale, with soil depth and slope position being two of the major drivers of SOC stock variability. The distribution of SOC stock varies with depth; SOC mostly occurs in the first meter of soil [42,43], while half of SOC stocks are stored in the first 30 cm for some of the major soil orders such as Entisols, Inceptisols, Alfisols, Ultisols, and Mollisols [44]. Additionally, the SOC stock closer to the surface is more sensitive to change because of land use and climate change [45]. Topography also plays a significant role in the spatial distribution of SOC stocks [21,24,46,47]. For example, prior work has [24] found that up to 70% of the variability in SOC contents could be explained by slope position. When considering slope, SOC is also impacted by erosion and the degree of soil water saturation [19], suggesting that drainage patterns influenced by topography also play a significant role.

The complexity of factors influencing the SOC stock amounts and distribution could present challenges for modeling spatial predictions. The methods for spatial predictions and the mapping of soil properties can generally be divided into two categories: geostatistical and conventional [48]. Geostatistical methods such as kriging can be combined with linear regression or advanced machine learning models such as random forest [49] or cubist models [43] to form hybrid models following regression kriging (RK) [50] principles. RK methods are usually multivariate and use environmental covariates to make continuous predictions between points. Thus, the limited number of samples with measured values such as carbon and their distribution impact the accuracy of the predictions, especially when using environmental covariates [51]. Adding to this challenge is the lack of reference samples as well as the heterogeneity of sampling methods [52–54]. The more traditional or conventional methods interpolate data between points based on tacit knowledge and models of soil formation [15,48] and spatially map properties based on polygons rather than grids, like most geostatistical methods. The US Soil Survey Geographic (gSSURGO) database is an example of a conventional soil mapping method based on climate, organisms or vegetation, parent material, and topography (clorpt) acting over time [13,15,48]. Both spatial prediction methods have their advantages and disadvantages. While polygon-based predictions are easy to interpret and may be accomplished with less point observations, they do not represent soil property distribution on a continuum, but are rather based on mean representative values (RV) assigned to an entire polygon or map unit [55]. Some polygon products also provide a range for the mean property values within the polygon and map units. For example, gSSURGO provides upper and lower limit values (UL and LL) for properties, which can be interpreted as the bounds of a confidence interval [56]. However, this is rather unique to the US gSSURGO and not necessarily true for all polygon-based products. On the other hand, geostatistical prediction methods represent the spatial distri-

bution of soil properties as a continuum, using grids where each pixel has a unique value and an uncertainty prediction, expressed often as the width of a confidence interval [48]. However, geostatistical methods are data-demanding, and when inadequate in density and distribution can affect prediction accuracy [55]. These models generally require validation data from measured values to be reliable [57].

Because of the diversity in predictive methods and factors associated with SOC stocks and their spatial prediction, as well as the amount and quality of the available measured data, the mapping of SOC stocks requires a multiscale approach. The objectives of this paper are: (i) to assess the variation in SOC stocks for the Fairview series at a field scale considering soil genetic horizons, land use and topographical factors; (ii) investigate the scalability of SOC stock predictions based on land use and land cover from the study site to the entire Fairview series spatial domain mapped based on gSSURGO; and (iii) monetarily quantify the uncertainties associated with the scalability of SOC stock predictions.

## 2. Materials and Methods

### 2.1. Study Site

This study site was the Piedmont Prairie restoration site and its surroundings located at the Reynolda Gardens in Winston-Salem, NC, USA (Lat/Long: 36°7'N, 80°16'W) (Figure 1). The prairie was established in 2014 in an area of approximately 5 hectares and is planted with 55 species of native forbs and grasses. Previously, the site was under management as a lawn and golf course. The prairie is surrounded by lawn grass and forest with predominately broadleaf deciduous trees (Figures 2 and 3). The major soil is the Fairview series located within the Major Land Resource Area (MLRA) 136, covering close to half a million hectares (436,148 ha) in Virginia and North Carolina (Figure 1). The soil is represented by one pedon with measured data located in central Arkansas in a forested site and outside of the MLRA 136. On the other hand, the location of our study site was within the extent of the Fairview series. The Fairview series is classified as fine, kaolinitic, mesic Typic Kanhapludults derived from residuum from felsic metamorphic or igneous rock [58]. This soil is very deep, well drained, and developed on slopes that vary from 2 to 60%, with surface elevation ranging between 245 and 265 m asl. The major land use for Fairview series comprises cultivated crops, pasture, and woodland. The annual average air temperature for the study area is 13.9 °C and the average annual precipitation is 112 cm [59].

### 2.2. Soil Sampling

The FAO's recommendations for measuring and modeling soil carbon stocks [60] were used to select the sampling sites. For the Piedmont prairie, 20 sites were selected using a conditioned Latin Hypercube (cLHC) [61] method based on the topographic position index, topographic wetness index, the relative slope position terrain attributes and elevation as covariates (Figure 2, Table 1). The topographic position index (TPI) classifies the altitude of each pixel against its neighboring pixels and is used for landform analysis [62]. If a pixel is higher in elevation than its surroundings, the TPI is positive, highlighting ridges and hilltops, or foot slopes if the pixel is lower in elevation than its surroundings pixels. The wetness index (TWI) is a measure of water surface runoff as guided by the surface terrain [63]. Higher values represent drier conditions with water running away, and lower values represent wetter conditions with water running towards the area or accumulating. Relative slope position numerically classifies the terrain in different positions along a slope gradient and is used in landform analysis and soil mapping [64]. Values vary from 0 to 1, with higher values indicating higher slope positions (i.e., ridges and summits) and lower values indicating lower positions (foot and toe slope). The cLHC method is a stratified random sampling procedure that selects samples based on the distributions of the values from gridded covariates. The sample size is set at the user's discretion, and through an optimization routine selects point values from the distribution of the covariates in the specified domain or covariate space [61]. If soil properties such as SOC correlate with covariates at the sampling locations, the sampling scheme allows for better and more

accurate predictions of soil property values for the unsampled grids in the specified domain or the covariate space.

UAS photogrammetry was used to generate a high-resolution digital elevation model (DEM). The meadow was mowed in winter and DJI Phantom 4 Pro UAS (DJI, Los Angeles, CA, USA) was flown on 1 May 2018, capturing imagery before the expansion of the warm season grasses. Flight was conducted at 60 m altitude using DroneDeploy control software v. 1.2.1 (DroneDeploy Inc., San Francisco, CA, USA) and images with a resolution of 1.6 cm GSD, 66% side lap, and 75% end lap. DEM was generated using Agisoft PhotoScan v1.4 (Agisoft LLC, St. Petersburg, Russia). Prior to deriving the terrain attributes, the DEM was resampled to a 0.5 m  $\times$  0.5 m grid using bilinear interpolation and smoothed using a majority filter (kernel size 2) to reduce noise. In addition, five sampling sites in the surrounding lawn and forest areas that represented dominant slope positions (summits, back slopes, and toe slopes) were selected. There was no available high-resolution DEM for the managed lawn and forest (Table 1); thus, the major slope positions were selected to capture those represented by the terrain attributes used for the Piedmont Prairie.

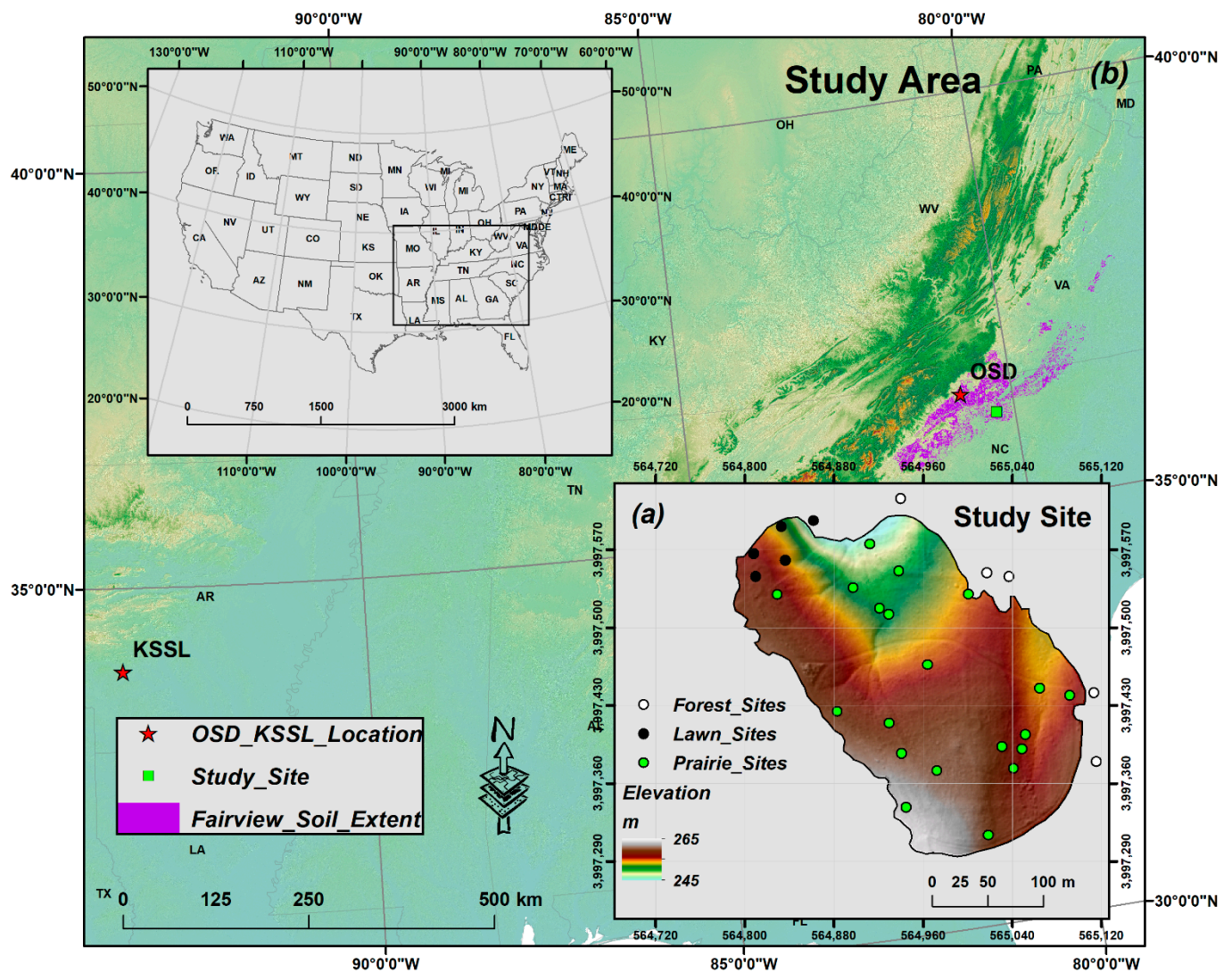


**Figure 1.** (a) Distribution of soil sampling points at the study site; (b) location of the study site and the spatial extent of the Fairview series in the study area showing the location of the official series description (OSD) and the pedon with laboratory analysis from the Kellogg Soil Survey Laboratory (KSSL).

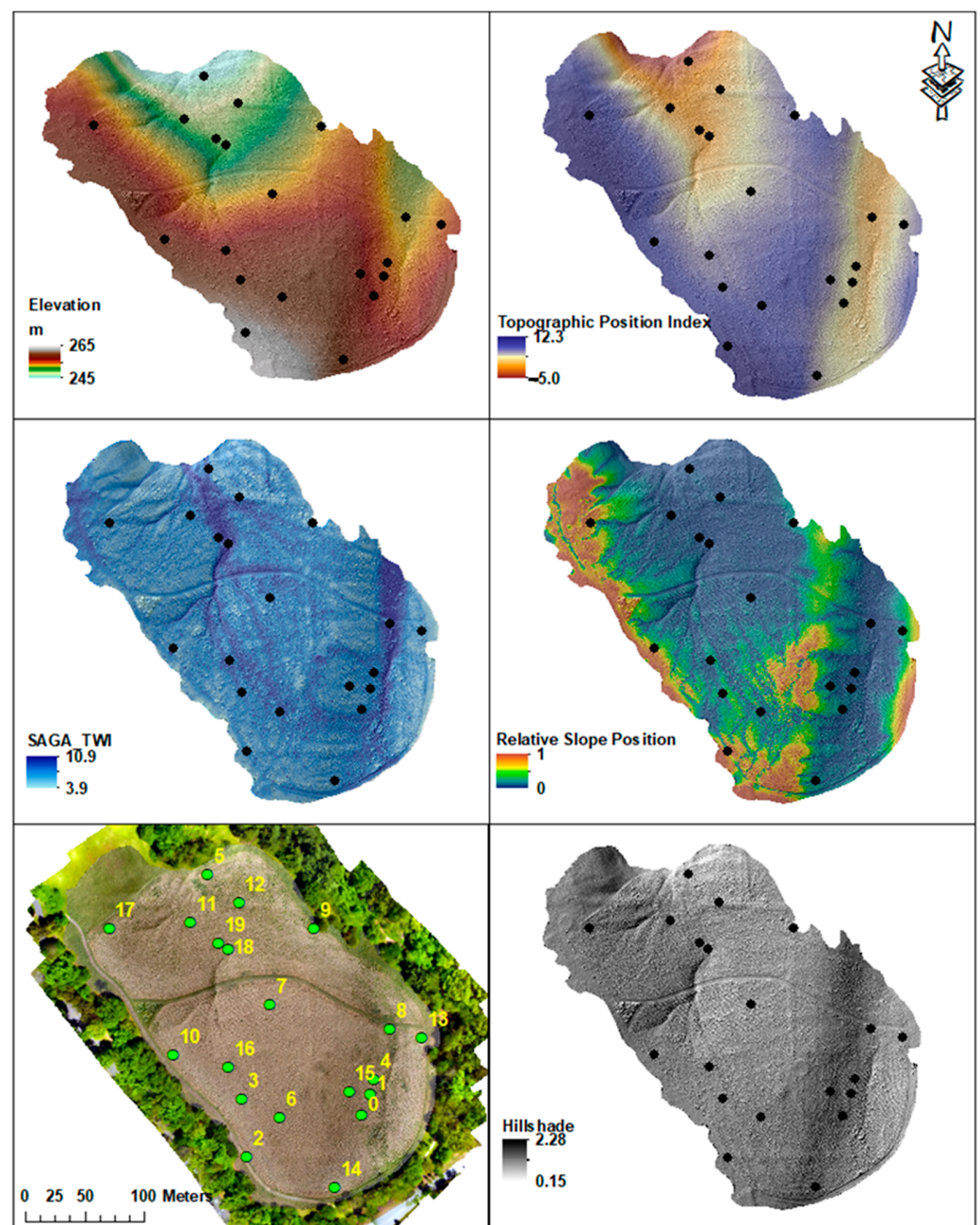


**Figure 2.** Elevation and terrain attributes of the study site derived from a digital elevation model (DEM) generated for locating sampling sites based on Latin hypercube conditions. Numbers represent the Sample ID (see Table 1).

**Table 1.** Terrain attributes and land use types by soil sampling points. Note that NA stands for not available.

Sample ID	Elevation (m)	Relative	Topographic		
		Slope Position	SAGA WI	Position Index	Land Use
Point 0	254.2	0.17	3.51	−0.77	Prairie
Point 1	254.1	0.03	4.58	−1.04	Prairie
Point 2	260.2	0.44	4.74	2.17	Prairie
Point 3	255.4	0	5.54	0.5	Prairie

Table 1. Cont.

Sample	Elevation	Relative	Topographic		
		Slope	SAGA	Position	Land
ID	(m)	Position	WI	Index	Use
Point 4	263.8	0.01	4.97	−1.12	Prairie
Point 5	245.8	0.02	5.99	−3.51	Prairie
Point 6	257.2	0.18	5.05	0.89	Prairie
Point 7	245.0	0	5.51	−0.36	Prairie
Point 8	249.5	0	6.67	−1.69	Prairie
Point 9	250.5	0.17	3.39	0.59	Prairie
Point 10	254.4	0.58	3.97	1.04	Prairie
Point 11	248.1	0.02	4.69	−2.14	Prairie
Point 12	248.2	0.06	4.08	−1.44	Prairie
Point 13	251.0	0.24	3.99	−0.4	Prairie
Point 14	254.6	0.14	4.5	−0.03	Prairie
Point 15	254.3	0.22	3.54	0.08	Prairie
Point 16	253.9	0.16	5.37	0.24	Prairie
Point 17	253.5	1.00	2.45	2.14	Prairie
Point 18	249.1	0	7.16	−2.08	Prairie
Point 19	249.0	0.01	6.77	−2.09	Prairie
Point 20	253.0	NA	NA	NA	Lawn Grass
Point 21	252.5	NA	NA	NA	Lawn Grass
Point 22	251.3	NA	NA	NA	Lawn Grass
Point 23	243.1	NA	NA	NA	Lawn Grass
Point 24	249.9	NA	NA	NA	Lawn Grass
Point 25	249.5	NA	NA	NA	Forest
Point 26	257.7	NA	NA	NA	Forest
Point 27	254.7	NA	NA	NA	Forest
Point 28	254.7	NA	NA	NA	Forest
Point 29	250.4	NA	NA	NA	Forest

### 2.3. Soil Analysis and SOC Stock Calculations

Soil samples were collected and described based on US Soil Survey standards and methods [65]. Three complete pedon descriptions and samples were conducted in each of the prairie, managed lawn, and forest areas (Figure 3). The remainder of the soil samples were collected by an auger to a depth of 0.5 m and were based on genetic horizons. At each site, three cores were taken inside a 0.5 m × 0.5 m plot and oven-dried at 110 °C for 24 h to determine bulk density [66].

Additional samples (2 in the forest and lawn areas, 17 in the prairie) were taken and composited for each genetic horizon, air-dried for 48 h, and ground to 2 mm for soil analysis. The soil samples were analyzed for organic carbon by the NC State Environmental and Agricultural Testing Services based on the dry combustion method. The soil organic carbon (SOC) stock (Mg ha<sup>−1</sup>) for the genetic horizon was calculated using Equation (1) for each of the sites for 0–50 cm soil thickness. During the field soil description and sampling processes, no rock fragments (RFs) were observed. Therefore, RFs were not included in Equation (1). The value of the SOC stocks (Mg ha<sup>−1</sup>) in USD was also calculated by multiplying the SOC stock with USD 30/Mg ha<sup>−1</sup> SOC value according to California Carbon Allowance stock prices [67].

$$\text{SOC (\%)} * \text{Bulk Density} \left( \frac{\text{g}}{\text{cm}^3} \right) * \text{Thickness (cm)} = \text{SOC Stocks} \quad (1)$$

During the field soil description and sampling processes, no rock fragments (RFs) were observed. Therefore, RFs were not included in Equation (1). The value of SOC stocks (Mg ha<sup>−1</sup>) in USD was also calculated by multiplying the SOC stock with USD 30/Mg ha<sup>−1</sup> SOC value according to California Carbon Allowance stock prices [67].

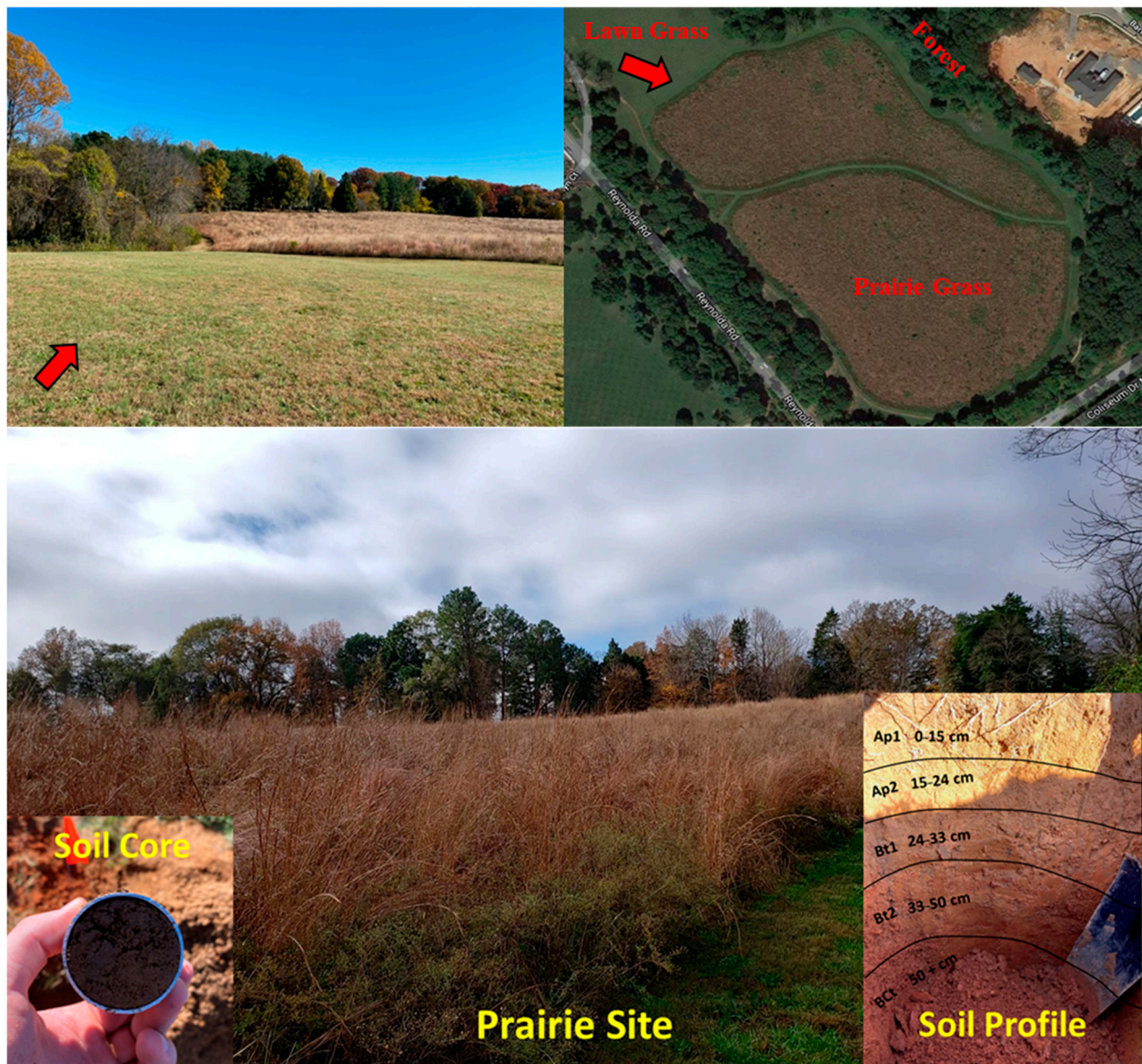


**Figure 3.** Soil landscape showing three different vegetation forms (prairie grass, lawn grass, and forest) with the lower left inset showing a soil core collected for determining the soil bulk density and a soil profile described and sampled.

#### 2.4. Spatial Modeling

The spatial prediction model was based on RK [68,69]. A regression between SOC stocks at sampling locations and topographic variables (elevation; topographic position index—TPI; SAGA wetness index—SAGA\_WI; and relative slope position—RSP) was performed using a multiple linear regression (MLR) model, and the model residuals were mapped using ordinary kriging (OK) and utilizing RStudio Team (2021) [70]. The selection of the specific terrain variables depended on their proven relationship with SOC distribution in the landscape [42,47,71]. RK modeling was performed separately for each genetic horizon (Ap, Bt and BC/C). The maps of the MLR-predicted SOC and OK residuals were summed together to yield the final spatial predicted maps. A residual variogram was modelled with 5 theoretical models (spherical—sph; exponential—exp; gaussian—gau; Mat: A model of the Matern family—mat; and M. Stein’s model—ste) [72], and the best fitting model was selected based on kappa statistics. The ste performed the best for all three horizons and was selected. The 90% confidence interval (CI) of the predicted SOC

for each horizon was also calculated. The  $z$ -value based on 18 degrees of freedom (19-1) and two tails with a  $p$ -value of 0.1 (90% CI) was 1.729. The 90% instead of 95% CI was considered more realistic given the uncertainty of natural systems compared to standard controlled experiments. Spatial modeling was only performed for the prairie grass due to lack of LiDAR coverage for the lawn grass and the forest.

### 2.5. Spatial Extrapolation to the Fairview Series

First, the amount of SOC stocks across Fairview series area was derived from the gSSURGO database [58] using the ArcMap-Soil Data Development Toolbox (Version date 13 October 2020). The tool is designed to utilize gSSURGO databases for creating soil property maps at user-specified depths. As the average soil thickness for the surface horizons in the study site was 25 cm, maps of SOC and Bd were generated for 0–25 cm before calculating the SOC stocks. The SOC stocks were estimated by means of the mentioned tool for a 0–25 cm soil depth. Furthermore, the lower and higher estimated SOC and Bd values across the soil series were extracted using the dominant component criteria. gSSURGO map units are polygons that can have more than one soil series or component mapped within the polygon boundaries. Fairview series was the major soil mapped in the study site; thus, the dominant component criterion was selected.

Second, an SOC stock map was also generated based on the gSSURGO Fairview soil series extent combined with the 2019 US Geological Survey LULC (<https://www.mrlc.gov/> (accessed on 1 April 2022)) map. The Fairview series area was overlaid with the USGS-LULC to determine the extent of forest, pasture, and managed lawns. The mean SOC and bulk density values from the forest, pasture, and managed lawns and their 90% CI at the study site were assigned to the gSSURGO Fairview series extent that corresponded to their respective USGS-LULC categories. The SOC stocks were calculated for the 0–25 cm soil thickness.

## 3. Results

### 3.1. Measured Values of Soil Organic Carbon and Bulk Density

Regardless of land use, the surface horizon (Ap) had an overall higher SOC content compared with the subsurface horizons (Bt or BC/C) (Table 2, Figure 4).

**Table 2.** Soil organic carbon (SOC, wt%), bulk density (Bd g cm<sup>−3</sup>), and SOC stock (Mg ha<sup>−1</sup>) sample mean ( $\bar{x}$ ), standard deviation ( $S_x$ ), and sample size ( $n$ ) for the pits and auger holes of the soil horizon.

Soil Characteristics	Horizon	Prairie Grass	Lawn Grass	Forest
		$\bar{x}$ ( $S_x, n$ )	$\bar{x}$ ( $S_x, n$ )	$\bar{x}$ ( $S_x, n$ )
Average Depth (cm)	Ap	26.33 (12.06, 3)	16.33 (3.51, 3)	11.83 (1.26, 3)
	Bt	13.00 (3.46, 3)	14.33 (2.89, 3)	18.75 (0.35, 2)
	BC	16.00 (2.82, 2)	19.33 (6.11, 3)	25.67 (10.79, 3)
Soil Organic Carbon (wt%)	Ap	1.88 (0.76, 20)	2.29 (1.39, 5)	2.59 (0.89, 5)
	Bt	0.67 (0.45, 20)	0.92 (0.32, 5)	0.85 (0.37, 5)
	BC	0.67 (0.32, 20)	0.61 (0.19, 5)	0.87 (0.59, 5)
Bulk Density (g cm <sup>−3</sup> )	Ap	1.19 (0.16, 12)	1.34 (0.11, 9)	0.96 (0.40, 9)
	Bt	1.51 (0.19, 9)	1.55 (0.13, 9)	1.32 (0.24, 6)
	BC	1.15 (0.28, 6)	1.21 (0.26, 9)	0.93 (0.24, 9)
SOC Stocks (Mg ha <sup>−1</sup> )	Ap	46.97 (14.70, 20)	47.88 (29.53, 5)	28.92 (9.69, 5)
	Bt	13.16 (8.55, 20)	20.39 (7.42, 5)	20.90 (7.65, 5)
	BC	18.59 (19.42, 20)	14.13 (5.79, 5)	23.04 (22.88, 5)

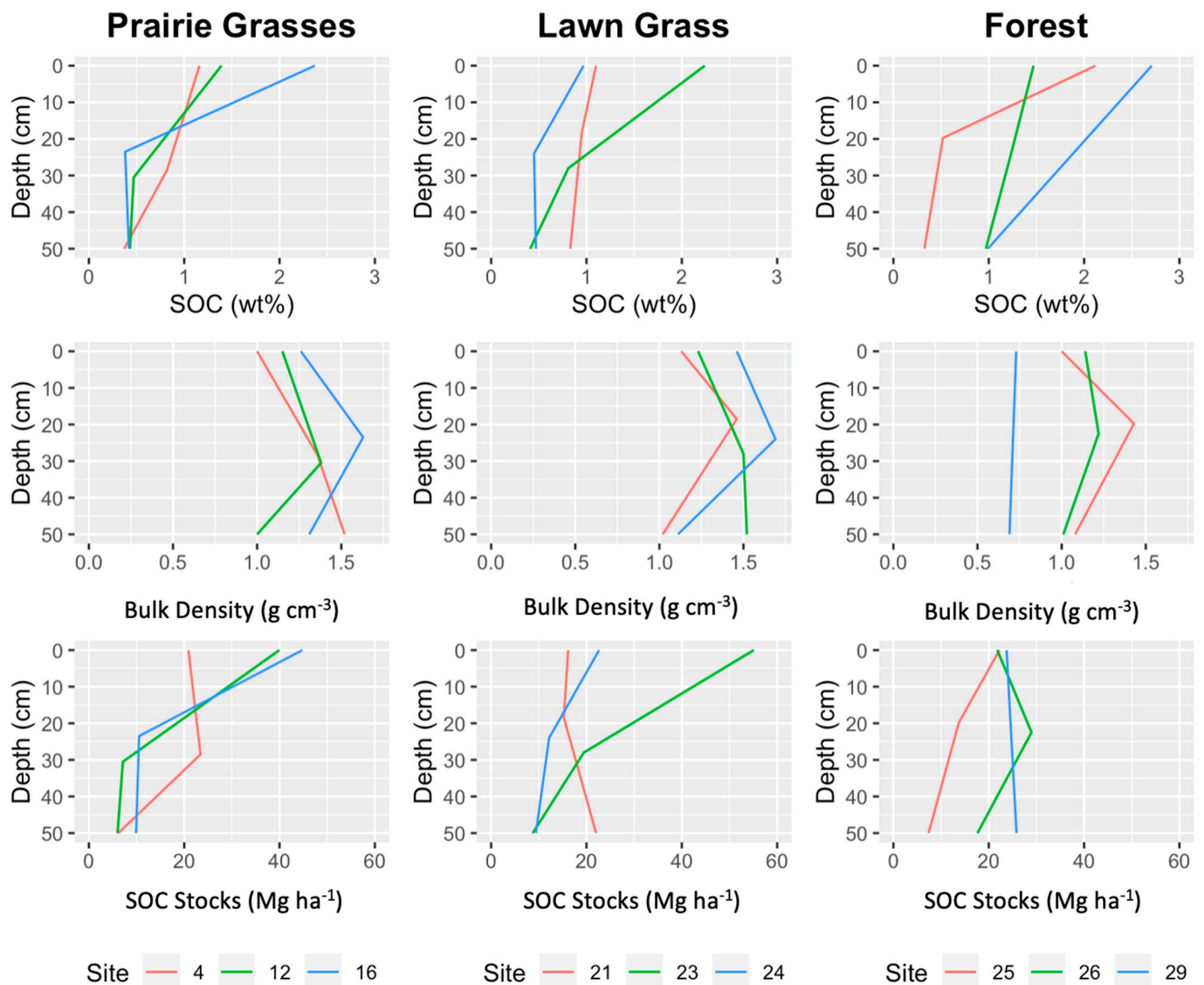


**Figure 4.** Distribution of SOC (wt%), Bd ( $\text{g}/\text{cm}^3$ ) and SOC stocks ( $\text{Mg}/\text{ha}$ ) with depth for soil pits in the prairie grass, lawn grass and forest.

The SOC content for Ap was twice as much compared to the subsurface horizons. The mean SOC content for the surface horizon of the lawn and forest were comparable, and higher than prairie. The soil bulk density, on the other hand, showed opposite trends between Ap and Bt, especially in terms of depth. The mean soil Bd for BC decreased and was comparable with the surface Bd regardless of land use.

### 3.2. SOC Stocks and Their Monetary Value

The prairie and lawn areas had more SOC stocks compared to the forest area, especially for the surface horizon. Prairie grass had significantly higher SOC stocks than forest, but only for the Ap horizon and only at  $p < 0.05$ . Additionally, lawn grass had significantly higher ( $p < 0.05$ ) SOC stocks compared to prairie for the Bt horizon. Overall, surface horizon had higher SOC stocks compared with the subsurface horizons (Table 2, Figure 5) across all land uses. However, not all the differences were significant for all land uses. The Ap horizon had significantly higher ( $p < 0.001$ ) SOC stocks compared to Bt and BC for prairie grass, while for lawn grass the Ap horizon had significantly higher ( $p < 0.05$ ) SOC stocks compared to BC.

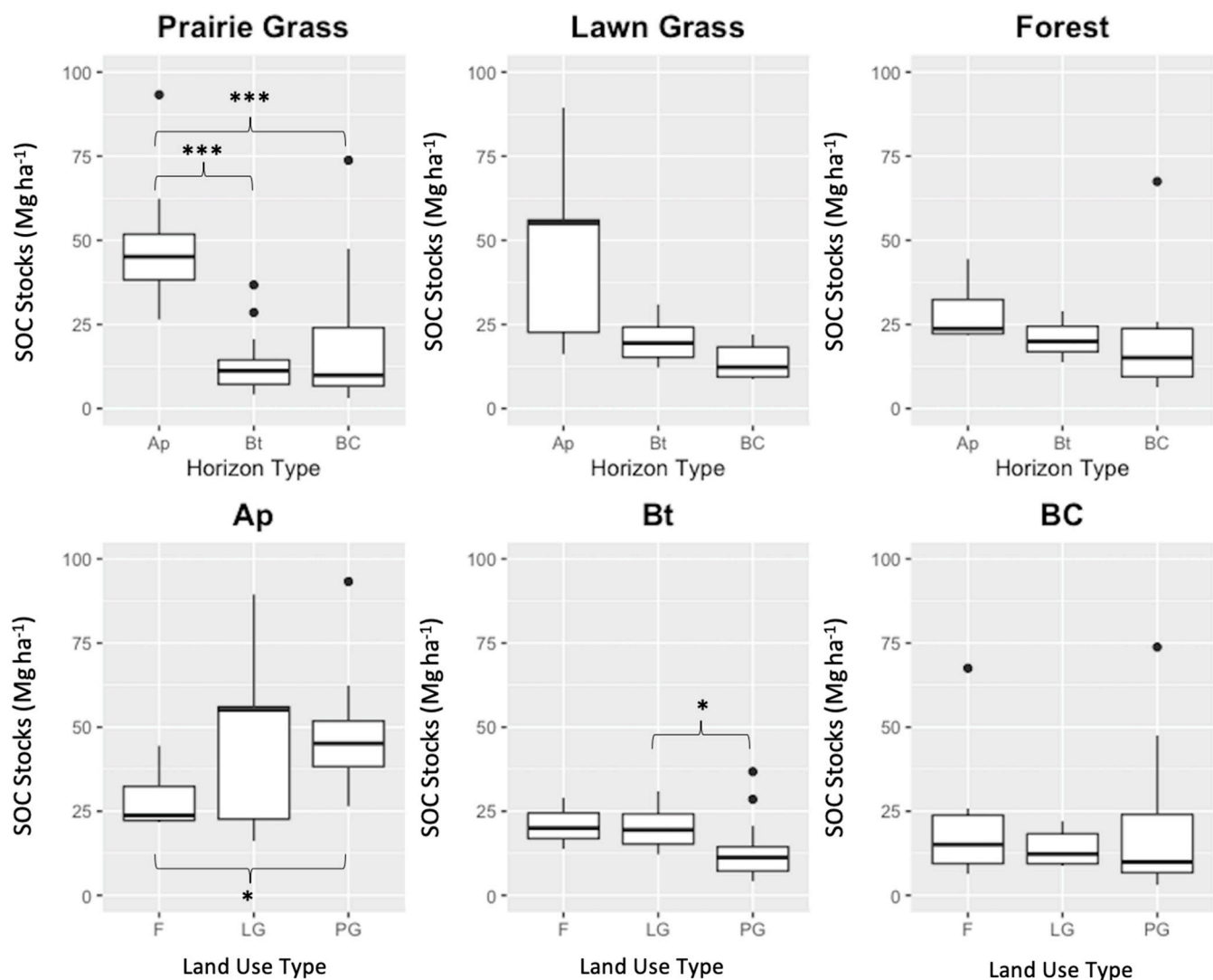


**Figure 5.** Box plots of mean SOC stock statistical comparisons by land use and soil horizons. Three stars indicate significance at  $p < 0.001$  and one star indicates significance at  $p < 0.05$ . black dots represent 5th and 95th percentile values.

The variability of SOC and Bd was high, especially for the surface horizon compared to the subsurface horizons. The SOC content was more variable for lawn grass compared to prairie grass and forest, as shown by the standard deviation values (Table 2). However, for Bd the opposite was true. The surface horizon was the least variable for lawn grass compared to prairie grass and forest. Like SOC content, the variability of SOC stocks was the highest for the Ap horizon for lawn grass compared to the other horizons across all land uses. Overall, the variability of SOC, Bd and SOC stocks decreased with depth between Ap and Bt, except for prairie grass and lawn grass, where variability for Bd slightly increased (Table 2).

### 3.3. SOC Stock Spatial Distribution for Prairie Grass

The MLR model was used to predict and map SOC stocks for each soil horizon from prairie area based on elevation, relative slope position (RSP), SAGA wetness index (SAGA-WI), and topographic position index (TPI) as predictors (Table 3). The RSP and TPI terrain attributes were the most influential on SOC stock predictions. While TPI was most influential for the Ap horizon, for Bt and BC, the RSP was most influential. Overall, elevation had a negative influence on SOC for all soil horizons, whereas TPI had a positive influence.

**Table 3.** Variogram parameters of the MLR model residuals, and RK cross validation results to predict SOC stocks.

	Parameters	Ap	Bt	BC
Variogram	Nugget	207.5	0.56	280.7
	Sill	258	29	261
	Range	4.8	48	306
	Kappa	0.3	0.4	0
Cross	R <sup>2</sup>	0.3	0.7	0.24
	ME	1.1	0.6	−3.7
	MAE	23.7	6.4	17.52
	RMSE	27.89	7.4	27.95
	p-value	0.23	0.004	0.56

The SOC stocks' MLR residuals for prairie grass showed spatial dependencies between neighboring sampling points, and varied in soil horizon (Table 3). The nugget/sill ratio was 80 and 100% for Ap and BC, indicating a weak spatial dependency according to the scale edified by a landmark prior study [73]. On the other hand, the nugget/sill ratio for the Bt horizon was only 2%, indicating a very strong spatial dependency and small degree of local variation, as also supported by the nugget value that was 0.56 compared to 207 and 280 for the Ap and BC horizons. The higher sill values for Ap (258) and BC (261) compared to Bt (29) suggest a higher variability between sampling points and lower prediction accuracy at finer scales. The strong spatial dependency and small local variation for the Bt were also reflected in the model's performance.

The distribution of SOC stocks for all horizons showed similar patterns. There were higher SOC stocks in the north–central and western parts of study area, and lower SOC stocks in the eastern part (Figure 6).

Higher SOC stocks were predicted for the summit with higher values of TPI and RSP, especially for the Bt horizons. The spatial pattern of SOC stock was similar among the horizons; however, there was more spatial variability for the Ap and BC horizons compared to Bt. The predicted SOC stock varied from 35.4 to 201.5 Mg ha<sup>−1</sup> for Ap and was higher overall compared to Bt and BC, which varied from 3.1 to 71.3 Mg ha<sup>−1</sup> and 1.0 to 109.7 Mg ha<sup>−1</sup>. The range of predicted SOC stock was larger compared to the range for the measured SOC stocks for all horizons. The uncertainty prediction of SOC expressed as the width of the 90% confidence interval was higher for the Ap horizon (12.3 to 57.4 Mg ha<sup>−1</sup>) compared to Bt (4.5 to 19.0 Mg ha<sup>−1</sup>) and BC (17.5 to 51.8 Mg ha<sup>−1</sup>). The uncertainty was higher for the summits compared to the back slope and toe slope positions.

The R<sup>2</sup> for the cross-validation of the regression kriging model was highest for Bt (0.7) and was significant ( $p = 0.004$ ) compared to Ap and BC. The mean absolute error (MAE) and root mean square error (RMSE) were also smaller for Bt compared to Ap and BC.

In terms of the extent of Fairview series in the MLRA 136, when using the estimated gSSURGO mean representative values (RV), the mean SOC stocks for the Fairview series ranged from 10 to 65 Mg ha<sup>−1</sup> (Figure 7). In terms of the difference in SOC stocks between estimated upper value (UV) and lower value (LV), the confidence interval proxy to the estimated RV, was from 2 to 65 Mg ha<sup>−1</sup> (Figure 7).

The difference between gSSURGO-estimated SOC stock based on RV and SOC stock based on measured values (Figure 7) ranged from 7 to 62 Mg ha<sup>−1</sup>. The SOC stock for the Fairview series area based on the combination of measured values from the study site and 2019 USGS-LULC ranged from 29 to 48 Mg ha<sup>−1</sup> (Figure 8) and the 90% confidence interval was between 11 and 56 Mg ha<sup>−1</sup> (Figure 8). The SOC stock difference between the gSSURGO estimated range (UV-LV) and the 90% CI based on the combination of the measured values from the study site and the USGS LULC ranged from −65 to 38 Mg ha<sup>−1</sup> (Figure 8).

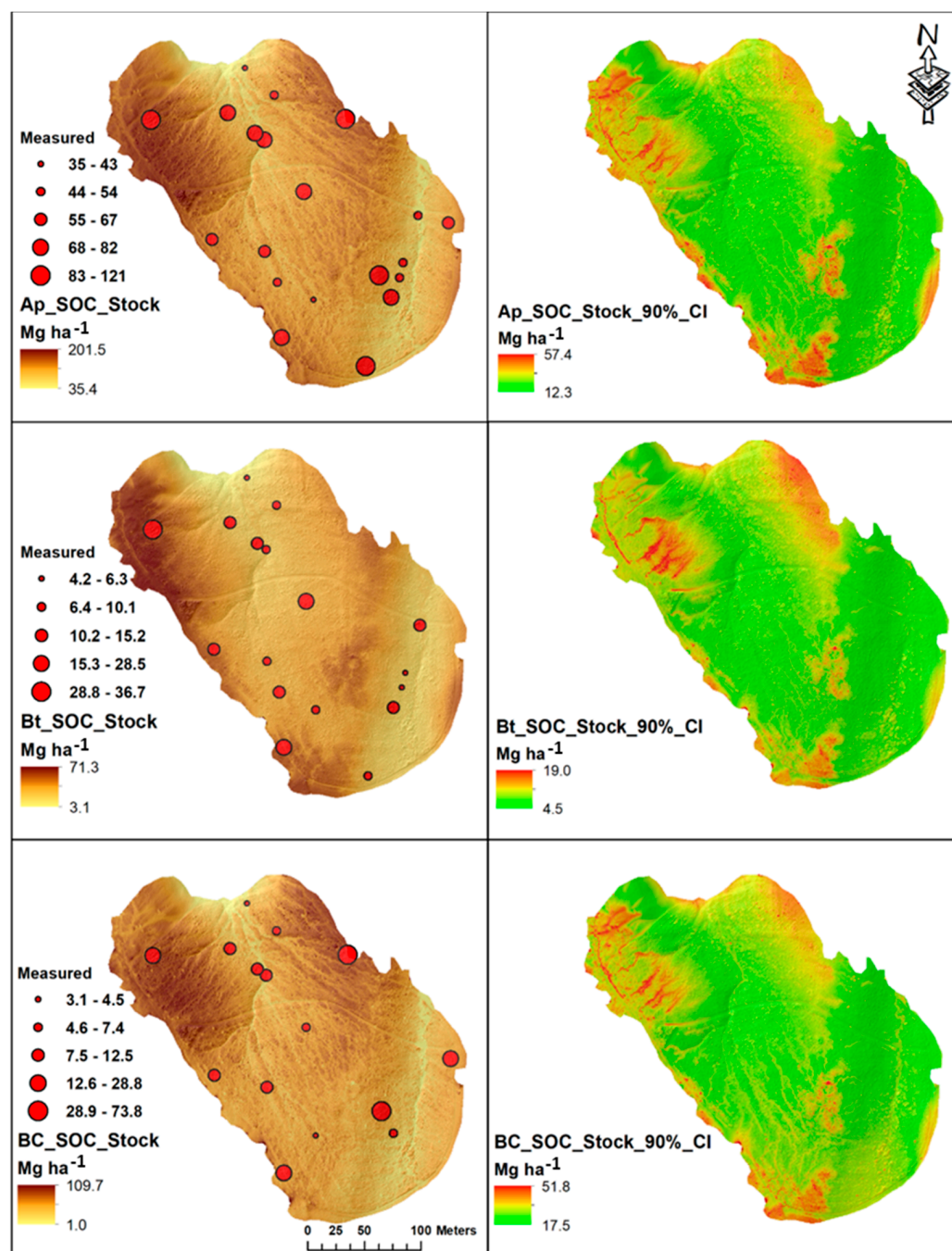


**Figure 6.** Spatial distribution of measured versus predicted SOC stocks (90% confidence interval, CI) for soil horizons on the prairie grass site.

However, when spatially subtracting the 90% CI width from gSSURGO (UV-LV), the difference varied from  $-17$  to  $46 \text{ Mg ha}^{-1}$ , suggesting that the uncertainty—as expressed by the 90% CI and gSSURGO UV-LV—was not spatially consistent and was either overestimated or underestimated in some of the areas (Figure 9).

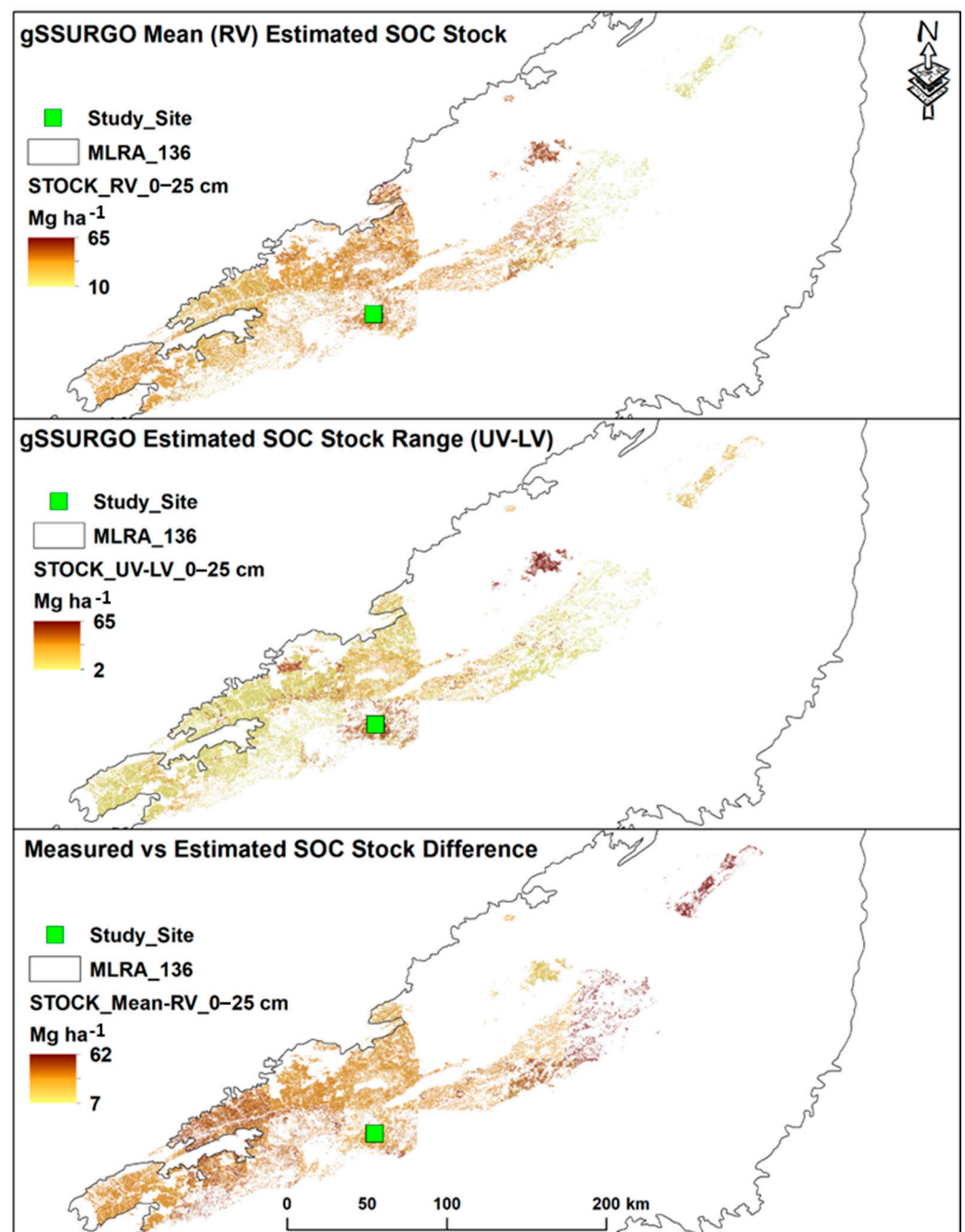


**Figure 7.** SOC stock distribution for the extent of the Fairview series in the study area for 0–25 cm soil thickness. The SOC stock was calculated as a mean based on the gSSURGO estimated representative value (RV) (**upper** panel) as the difference between the estimated upper values (UV) and the lower values (LV) (**middle** panel). The **lower** panel shows the difference between the measured and estimated SOC stock values.

The 90% CI was narrower for the prairie ( $10.6 \text{ Mg ha}^{-1}$ ) and forest ( $14.6 \text{ Mg ha}^{-1}$ ) areas. In order to better assess the impact of the differences in SOC stock between land uses, the uncertainty was expressed in USD/Mg stock. Converted to USD per  $\text{Mg ha}^{-1}$  SOC stock (assuming USD 30/ $\text{Mg ha}^{-1}$  SOC stock, based on California Carbon Allowance stock prices) the uncertainty for the gSSURGO using the difference between UV-LV was USD  $1890 \text{ ha}^{-1}$ , and thus comparable with the 90% CI for the lawn grass (USD  $1689 \text{ ha}^{-1}$ ). The uncertainty levels for prairie and forest areas were smaller, with USD  $10.6 \text{ ha}^{-1}$  and USD  $14.6 \text{ ha}^{-1}$  compared to lawn grass and the gSSURGO.

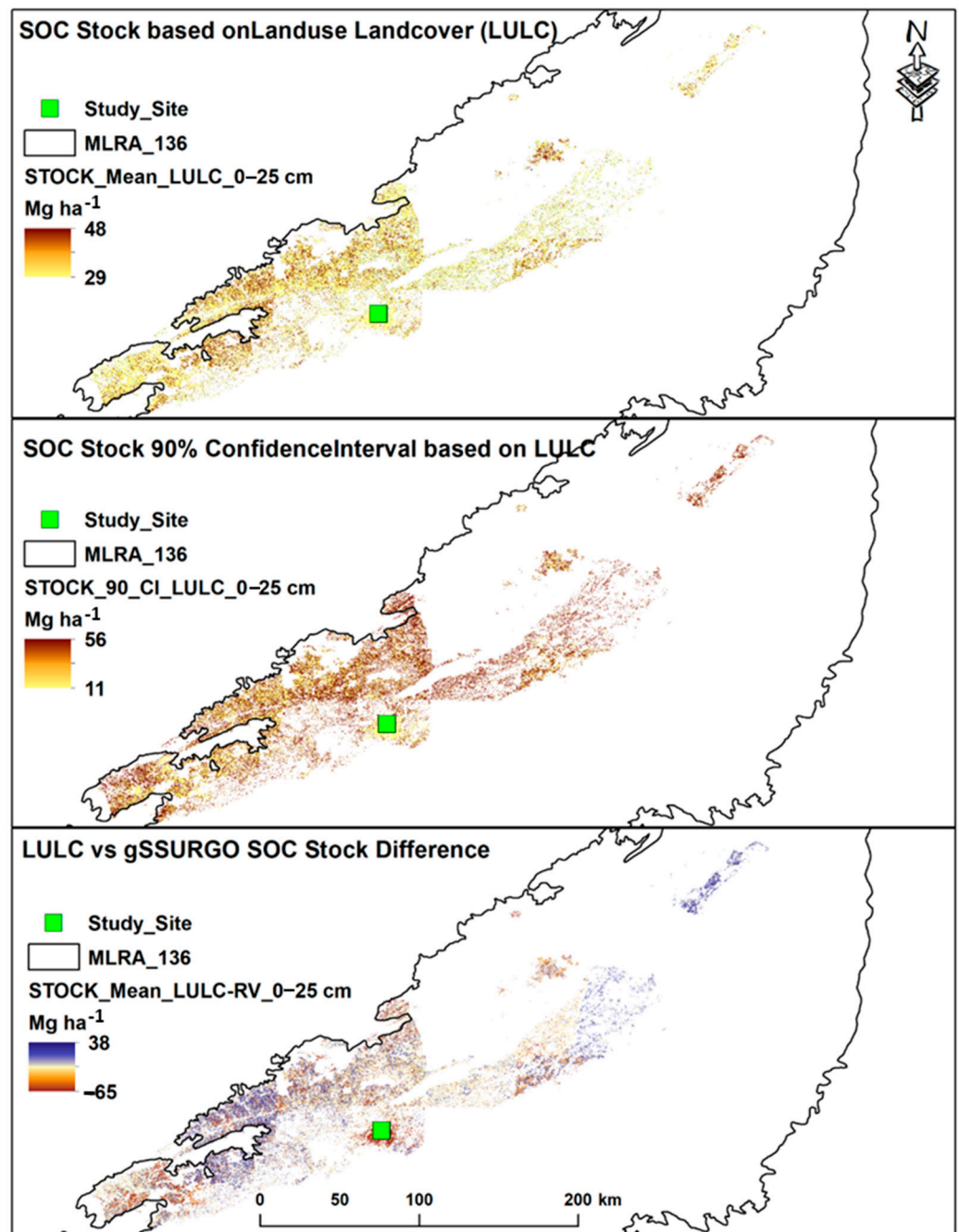


**Figure 8.** Mean SOC stock distribution at a regional level for the Fairview series area (including the study area), based on measured values from prairie grass, lawn grass and forest sites, assigning the 2019 USGS-LULC categories (**upper** panel), 90% confidence interval for the mean SOC stock (**middle** panel), and the difference between the mean SOC stock calculated based on 2019 USGS-LULC and the gSSURGO-RV.

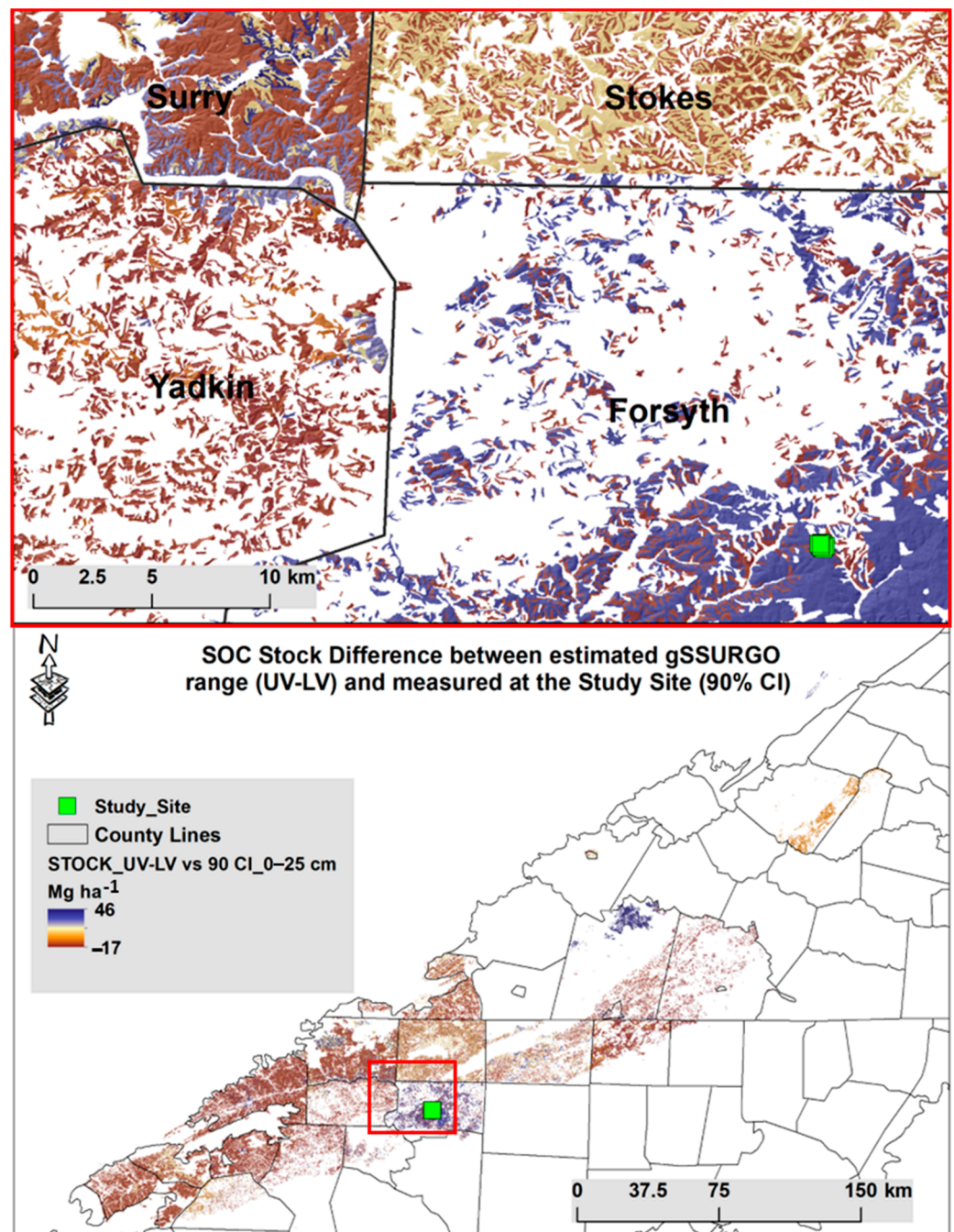


**Figure 9.** Spatial distribution of SOC stock difference between the estimated gSSURGO range (UV-LV) and the calculated range (90% CI) at the study site based on the measured values for the Fairview series. The upper panel offers a closer look at the contrast between the administrative boundaries and the difference between the two measures of the CI (UV-LV-estimated CI versus 90% CI from measured values for 0–25 cm soil thickness).

#### 4. Discussion

The differences in mean SOC stock based on measured or estimated values, as well as their respective prediction ranges (90% CI and UV-LV), were comparable in trend and magnitude. However, there were spatial differences both locally (study site level) and regionally (MLRA level). There may be many factors for these differences, such as land use and management [13,37,74], modelling (gSSURGO or geostatistical bases) [50,55,75], and measurement methods [76], among others. First, we focus on the local spatial variability of

the study site followed by a discussion at MLRA level and conclude with some remarks on uncertainty interpretations.

#### 4.1. Land Use Effects with Soil Depth on SOC Stocks

The SOC stocks at the study site varied both spatially and in depth, but mostly in terms of surface horizon (Figures 4 and 6). Additionally, most of the stock—between 40 and 60%—was concentrated on the surface horizons (0–25 cm), except for the forest where the amount of stock for the surface layer was comparable with the subsurface (Table 2). The distribution of SOC stock with depth may be related to land use [77,78] and the dynamics of the study site, as found elsewhere [79]. Multiple land use changes in the original broadleaf forest, located there since European settlement, may have occurred at the study site, which may have led to the redistribution of SOC stocks and altered depths, especially for the forest area [80]. Prior research has shown that the changing of land use practices can lead to significant differences in soil properties and thickness [32–34]. Given the replanting and conversion of the site in the last half century, it would be expected that soil thickness, and especially SOC in the top horizon, would vary significantly. On the other hand, the relatively sharp decline in stock with depth for both the prairie and lawn areas in comparison to the forest may also be related to the relatively new prairie establishment (5 years) and management of the lawn. Studies have shown that, initially, the accumulation rate of SOC for deeper layers under native prairie is slower compared to managed crop rotation systems [81], leading to more SOC at the surface layer. Though over extended periods of time (i.e., thousands of years) SOC moves down the land profile, leading to SOC-enriched soil profiles, on a decadal scale, most of the SOC could still remain in the 0–40 cm depth [82–84], driven mainly by root distribution, which plays a significant role in SOC content distribution with depth [85]. According to Equation (1), the distribution of SOC stocks with depth is related to SOC content and Bd. Data from our study showed that the stock change with depth was driven more by the SOC concentration than Bd, a finding corroborated by another study [86]. The SOC content decreased at similar rates (Ap to Bt) regardless of the land use. However, the SOC stock decrease was lesser for the forest compared to the prairie and lawn areas, mostly due to the difference in bulk density. The Bd for the prairie and lawn areas increased with depth (Ap to Bt) by approximately 1 time, but by 1.4 times for the forest. On the other hand, the SOC concentration was, overall, 2.8 times higher for Ap than Bt across all land uses, with the forest having the highest value (3.1). The SOC stock was 2.2 times higher for Ap compared to Bt with prairie grass having the highest difference (2.9) and forest the lowest (1.4). Additionally, the SOC concentration and stock were more variable compared to Bd, as observed by others [86,87]. Higher SOC stock variability and concentration for the surface horizon compared to subsurface horizons have been reported by other researchers as well [42,88,89].

Another variability factor is related to the spatial distribution of SOC stock as influenced by terrain [85]. Overall, more SOC stock was found on summits compared to back slope and toe slope. Erosion, whether natural or anthropogenic, is a well-recognized process that erodes the accumulated surface SOC and transports and deposits it downstream [46,85,90]. Thus, the higher SOC content and stock at the summit reflects the stability of this slope position with regard to erosion. However, the relationship between SOC and slope position depends on the characteristics of the landscape [24]. A study from the lower Himalayas in India found higher amounts of SOC stock at the summits and back slopes compared to toe slopes [91], in part due to the summits and back slopes being more resistant to erosion than the toe slopes. However, other studies found the opposite, with higher SOC stocks in the lower back slopes and toe slopes compared to the summit [20,23]. The watershed size and the location of the study site within the watershed likely explain the opposite trends compared to our study site. Both studies [20,23] focus on larger watersheds where the distribution of precipitation and runoff can have a larger influence on soil organic carbon distribution in the landscape, especially downstream. An Iowa watershed [21] found that toe slopes and foot slopes predominated in terms of SOC stocks relative to back

slopes, and the researchers attributed this to the combined effect of soil erosion and SOC deposition within watersheds. In riparian soil profiles [1,22], significantly larger deposits of SOC stocks were found compared to upland soil profiles, which could further explain the distinction between the soil profiles of upland soils and watersheds. Our study site was located on a hillslope with a small first-order stream and away from major downstream tributaries, with larger contributing areas and erosion and deposition rates as a result.

#### 4.2. Spatial Prediction and Extrapolation Uncertainty

The strong relationship between terrain attributes and Bt, and the subsequent better performance of regression kriging seem to suggest that the argillic horizon is better preserved compared to the surface horizon (Ap) and deeper horizon (BC). SOC stock calculations can be based on fixed depth increments or genetic horizons, and the choice often reflects the data and scale of mapping [13,74,92]. Global and regional models that may rely on multiple data sources prefer fixed depth increments. The selection is dictated, in most cases, by the incompatibility of data gathering protocols from various sources, as shown by multiple modeling efforts [50,75,93]. However, the fixed depth approach may not fully capture the relationships between pedogenesis, soil landscape, and SOC stock dynamics [94] and, furthermore, may not be sensitive to land use comparisons [79]. The significant differences between surface and subsurface horizon and between land uses, especially for the surface horizon in our study site, further support the importance of genetic horizons for SOC stock trend evaluation, especially at field level. The poor modeling performance for the Ap could likely be attributed to management that has influenced the relationship between SOC stock and terrain. Similarly, we postulate that the SOC stock for the BC horizon was less influenced by management and terrain and more by parent material and depth; thus, it did not show a good correlation with topography. On the other hand, the better model performance for the Bt horizon suggests that this pedogenic horizon better preserves landscape and topography compared to the other horizons.

Despite the geographic distance of the Fairview pedon from the study site, the measured SOC content and Bd were comparable with the values measured at the study site (Tables S2 and S3). For example, the pedon SOC content was 3.3% for the Ap horizon and decreased to less than 0.5% for the subsurface horizons. The SOC amount (2.6%) and depth trends were comparable and similar to the study site, especially for the forest. Similarly, the pedon Bd increased from 1.30 to 1.87 g cm<sup>-3</sup> between the surface and subsurface horizons, which was similar with the prairie and lawn areas. On the other hand, the forest showed similar trends, but the Bd was lower for the surface (0.96 g cm<sup>-3</sup>). The values for SOC and Bd between the pedons and the study site and between the pedons and the gSSURGO estimations were similar, leading to comparable mean SOC stocks and confidence intervals. The SOC stock difference between the estimated upper and lower values, a measure of uncertainty as shown by a previous study [56], was 63 Mg ha<sup>-1</sup> and comparable with a 90% CI for the lawn grass (56 Mg ha<sup>-1</sup>). Interestingly, the difference between the pedon mean-measured KSSL and gSSURGO estimate for the 0–25 cm soil thickness was USD 1650 ha<sup>-1</sup> and comparable with lawn grass and the gSSURGO (UV-LV). However, there were differences in the spatial distribution of the confidence intervals between the gSSURGO estimates and the measured values from the study site when applied to the Fairview series extent in MLRA 136. The 90% CI for the measured SOC stock from the study site in combination with the 2019 USGS-LULC for the Fairview series extent in MLRA 136 was between 11 and 56 Mg ha<sup>-1</sup>. This was slightly narrower compared to gSSURGO UV-LV, which was between 2 and 65 Mg ha<sup>-1</sup>. In addition, the spatial difference showed artifacts related to administrative boundaries. These inconsistencies are not surprising, given the fact that the soil surveys which are the foundation of the gSSURGO were conducted at different times by different surveyors using evolving technology and software [55], leading to uncertainties varying both in scale and direction [95–97].

Although the uncertainty of the prairie and forest areas were small relative to lawn grass and gSSURGO, when expressed in monetary terms and applied to the Fairview

extent in MLRA 136, even the smallest uncertainty could translate to large amounts of money. For example, the smallest uncertainty was  $2.5 \text{ Mg ha}^{-1}$  for the difference between Bd determined at field capacity (33 kPa) and oven-dried (OD). However, when expressed in relation to the Fairview series extent, this translates to approximately USD 33 million. The  $56.3 \text{ Mg ha}^{-1}$  uncertainty for lawn grass from the study site was worth approximately USD 737 million, but was less for the prairie (USD 139 million) and forest areas (USD 191 million) (Figure 10).

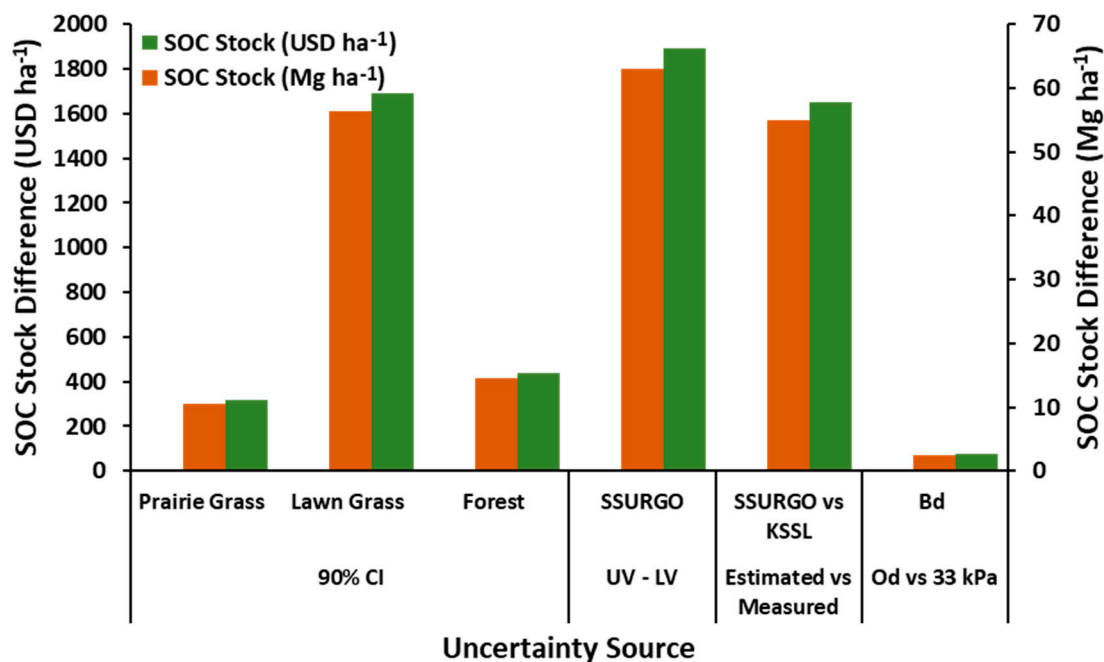


**Figure 10.** Differences in SOC stocks ( $\text{Mg ha}^{-1}$ ) and SOC stock value ( $\text{\$ ha}^{-1}$ ) for different uncertainty sources for the Fairview series.

The uncertainty due to gSSURGO (UV-LV) and the difference between gSSURGO and measured pedon (KSSL) were among the largest amounts: USD 824 and USD 720 million, respectively. The intensive management of the lawn grass relative to both the prairie and forest areas, and the field's historical land use changes—from forested, to a golf course, to turf grass—seem to be reasonable explanations for the observed increased uncertainty in the lawn grass, as found by others [1,2,8,75,86]. Studies focused on land management and ecology have found that, in heavily managed landscapes, anthropogenic drivers will come to dominate natural ones [38,98].

## 5. Conclusions

In this study we combined several data types, scales, and forms of analysis that formed this unique approach. We used LiDAR in combination with measured ground data and existing regional soil data to assess SOC stock variability in relation to factors such as land use, topography, and soil depth. Furthermore, we utilized land use data collected from satellite imagery to upscale the SOC stocks to the full geographic extent of the major soil found in the study area. Finally, we estimated the uncertainty related to the evaluation and upscaling of SOC from a monetary perspective, highlighting some of the challenges in an accurate account of SOC stocks.

The SOC stock distribution depth was influenced by land use and topography. The SOC stock was higher for the surface horizons compared to the subsurface horizons, and higher for the summits compared to the backslope and the footslope. The SOC stock uncertainty prediction ranges based on gSSURGO estimates and measured values were comparable. However, the distribution of the uncertainty prediction ranges was spatially inconsistent between the gSSURGO estimates and the measured values for the Fairview

soil series extent. Spatially, the SOC stock uncertainty was over or underestimated by gSSURGO relative to stocks determined based on measured SOC and upscaled to the Fairview extent based on the 2019 USGS-LULC at the study site. Assessing and upscaling accuracy predictions from a site to a larger area is challenging due to both the influence of environmental controls at a local scale, such as land use and topography, and differences between data sources at larger scales.

**Supplementary Materials:** The following supporting information can be downloaded at: <https://www.mdpi.com/article/10.3390/rs14122846/s1>, Table S1: SOC stock comparisons between soil horizons by land use cover (LULC) and between LULC by soil horizon; Table S2: Soil properties and calculated SOC stocks based on pedon-measured values from the KSSL; Table S3: Mean SOC stocks, 90% confidence intervals (90% CI) and estimates between gSSURGO upper values (UV) and lower values (LV).

**Author Contributions:** Conceptualization and project administration: K.W.B., M.R.S. and Z.L.; methodology: K.W.B., M.R.S., C.K. and Z.L.; data collection: K.W.B. and X.M.; data analysis: K.W.B., K.A. and Z.L.; writing and review: K.W.B., K.A., M.R.S., C.K., X.M. and Z.L. All authors have read and agreed to the published version of the manuscript.

**Funding:** This research received no external funding.

**Data Availability Statement:** The data used for this study is provided in Supplemental Materials Tables S1–S3.

**Acknowledgments:** The authors would like to thank Reynolda Gardens in Winston-Salem, NC for allowing us to use their prairie grass land for the study site. Additionally, the authors would like to thank the undergraduate and graduate students in the lab of Miles Silman for their input and advice, as well as the WFU Center for Energy, Environment, and Sustainability. Finally, we would like to thank both the USDA and NC State's Environmental and Agricultural Testing Service for their assistance. Zamir Libohova is a member of Research Consortium GLADSOILMAP, supported by LE STUDIUM Loire Valley Institute for Advanced studies. USDA is an equal opportunity provider and employer.

**Conflicts of Interest:** The authors declare no conflict of interest.

## References

- Hillel, D.; Rosenzweig, C. Soil Carbon and Climate Change: Carbon Exchange in the Terrestrial Domain and the Role of Agriculture. *Crop. Soils* **2009**, *5*, 5–10.
- Matson, P.A.; Parton, W.J.; Power, A.G.; Swift, M.J. Agricultural Intensification and Ecosystem Properties. *Science* **1997**, *277*, 504–509. [[CrossRef](#)] [[PubMed](#)]
- Six, J.; Paustian, K. Aggregate-Associated Soil Organic Matter as an Ecosystem Property and a Measurement Tool. *Soil Biol. Biochem.* **2014**, *68*, A4–A9. [[CrossRef](#)]
- Stott, D.; Kennedy, A.; Cambardella, C. Impact of Soil Organisms and Organic Matter on Soil Structure. In *Soil Quality and Soil Erosion*; Lal, R., Ed.; CRC Press: Boca Raton, FL, USA, 1999; pp. 57–74.
- Lal, R. Carbon Sequestration. *Philos. Trans. R. Soc. B Biol. Sci.* **2008**, *363*, 815–830. [[CrossRef](#)] [[PubMed](#)]
- Lal, R. Climate Change and Food Security Soil Carbon Sequestration Impacts on Global. *Science* **2004**, *304*, 1623–1627. [[CrossRef](#)] [[PubMed](#)]
- Metz, B.; Davidson, O.; Bosch, P.; Dave, R.; Meyer, L. *Contribution of Working Group III to the Fourth Assessment Report of the IPCC. Climate Change 2007 Mitigation of Climate Change*; IPCC: Geneva, Switzerland, 2007; ISBN 978-0521-88011-4.
- Houghton, J.T.; Ding, Y.; Griggs, D.J.; Noguer, M.; van der Linden, P.J.; Dai, X.; Maskell, K.; Johnson, C.A. *Climate Change 2001: The Scientific Basis. Contribution of Working Group I to the Third Assessment Report of the IPCC*; Cambridge University Press: New York, NY, USA, 2001; ISBN 0521-80767-0.
- Masson-Delmotte, V.; Zhai, P.; Chen, Y.; Goldfarb, L.; Gomis, M.I.; Matthews, J.B.R.; Berger, S.; Huang, M.; Yelekçi, O.; Yu, R.; et al. *Climate Change 2021: The Physical Science Basis. Working Group I Contribution to the Sixth Assessment Report of the IPCC*; Cambridge University Press: New York, NY, USA, 2021; ISBN 978-92-9169-158-6.
- Lal, R.; Kimble, J.; Follett, R.; Cole, C. *The Potential of US Cropland to Sequester Carbon and Mitigate the Greenhouse Effect*; CRC Press LLC: Boca Raton, FL, USA, 1999.
- Minasny, B.; Malone, B.P.; McBratney, A.B.; Angers, D.A.; Arrouays, D.; Chambers, A.; Chaplot, V.; Chen, Z.S.; Cheng, K.; Das, B.S.; et al. Soil Carbon 4 per Mille. *Geoderma* **2017**, *292*, 59–86. [[CrossRef](#)]

12. Soussana, J.F.; Lutfalla, S.; Ehrhardt, F.; Rosenstock, T.; Lamanna, C.; Havlík, P.; Richards, M.; Wollenberg, E.; Chotte, J.L.; Torquebiau, E.; et al. Matching Policy and Science: Rationale for the ‘4 per 1000—Soils for Food Security and Climate’ Initiative. *Soil Tillage Res.* **2019**, *188*, 3–15. [\[CrossRef\]](#)
13. Adhikari, K.; Owens, P.R.; Libohova, Z.; Miller, D.M.; Wills, S.A.; Nemecek, J. Assessing Soil Organic Carbon Stock of Wisconsin, USA and Its Fate under Future Land Use and Climate Change. *Sci. Total Environ.* **2019**, *667*, 833–845. [\[CrossRef\]](#)
14. Burke, I.C.; Yonker, C.M.; Parton, W.J.; Cole, C.V.; Flach, K.; Schimel, D.S. Texture, Climate, and Cultivation Effects on Soil Organic Matter Content in U.S. Grassland Soils. *Soil Sci. Soc. Am. J.* **1989**, *53*, 800–805. [\[CrossRef\]](#)
15. Jenny, H. Factors of Soil Formation, a System of Quantitative Pedology. *Agron. J.* **1941**, *33*, 857–858. [\[CrossRef\]](#)
16. Kern, J.S. Spatial Patterns of Soil Organic Carbon in the Contiguous United States. *Soil Sci. Soc. Am. J.* **1994**, *58*, 439–455. [\[CrossRef\]](#)
17. Parton, W.J.; Schimel, D.S.; Cole, C.V.; Ojima, D.S. Analysis of Factors Controlling Soil Organic Matter Levels in Great Plains Grasslands. *Soil Sci. Soc. Am. J.* **1987**, *51*, 1173–1179. [\[CrossRef\]](#)
18. Guillaume, T.; Makowski, D.; Libohova, Z.; Bragazza, L.; Sallaku, F.; Sinaj, S. Soil Organic Carbon Saturation in Cropland-Grassland Systems: Storage Potential and Soil Quality. *Geoderma* **2022**, *406*, 115529. [\[CrossRef\]](#)
19. Da Silva, A.P.; Nadler, A.; Kay, B.D. Factors Contributing to Temporal Stability in Spatial Patterns of Water Content in the Tillage Zone. *Soil Tillage Res.* **2001**, *58*, 207–218. [\[CrossRef\]](#)
20. Li, Y.; Zhang, Q.W.; Reicosky, D.C.; Bai, L.Y.; Lindstrom, M.J.; Li, L. Using <sup>137</sup>Cs and <sup>210</sup>Pbex for Quantifying Soil Organic Carbon Redistribution Affected by Intensive Tillage on Steep Slopes. *Soil Tillage Res.* **2006**, *86*, 176–184. [\[CrossRef\]](#)
21. Moorman, T.B.; Cambardella, C.A.; James, D.E.; Karlen, D.L.; Kramer, L.A. Quantification of Tillage and Landscape Effects on Soil Carbon in Small Iowa Watersheds. *Soil Tillage Res.* **2004**, *78*, 225–236. [\[CrossRef\]](#)
22. Ritchie, J.C.; McCarty, G.W. <sup>137</sup>Cesium and Soil Carbon in a Small Agricultural Watershed. *Soil Tillage Res.* **2003**, *69*, 45–51. [\[CrossRef\]](#)
23. Pierson, F.B.; Mulla, D.J. Aggregate Stability in the Palouse Region of Washington: Effect of Landscape Position. *Soil Sci. Soc. Am. J.* **1990**, *54*, 1407–1412. [\[CrossRef\]](#)
24. Thompson, J.A.; Kolka, R.K.; Thompson, J.A. Soil Carbon Storage Estimation in a Forested Watershed Using Quantitative Soil-Landscape Modeling. *Soil Sci. Soc. Am. J.* **1990**, *69*, 1086–1093. [\[CrossRef\]](#)
25. Conant, R.T.; Ryan, M.G.; Ågren, G.I.; Birge, H.E.; Davidson, E.A.; Eliasson, P.E.; Evans, S.E.; Frey, S.D.; Giardina, C.P.; Hopkins, F.M.; et al. Temperature and Soil Organic Matter Decomposition Rates—Synthesis of Current Knowledge and a Way Forward. *Glob. Chang. Biol.* **2011**, *17*, 3392–3404. [\[CrossRef\]](#)
26. Jobbágy, E.G.; Jackson, R.B. The Vertical Distribution of Soil Organic Carbon and its Relation to Climate and Vegetation. *Ecol. Appl.* **2000**, *10*, 423–436. [\[CrossRef\]](#)
27. Follett, R.F.; Stewart, C.E.; Pruessner, E.G.; Kimble, J.M. Effects of Climate Change on Soil Carbon and Nitrogen Storage in the US Great Plains. *J. Soil Water Conserv.* **2012**, *67*, 331–342. [\[CrossRef\]](#)
28. Battle-Bayer, L.; Batjes, N.H.; Bindraban, P.S. Changes in Organic Carbon Stocks upon Land Use Conversion in the Brazilian Cerrado: A Review. *Agric. Ecosyst. Environ.* **2010**, *137*, 47–58. [\[CrossRef\]](#)
29. Muñoz-Rojas, M.; Jordán, A.; Zavala, L.M.; de la Rosa, D.; Abd-Elmabod, S.K.; Anaya-Romero, M. Impact of Land Use and Land Cover Changes on Organic Carbon Stocks in Mediterranean Soils (1956–2007). *Land Degrad. Dev.* **2015**, *26*, 168–179. [\[CrossRef\]](#)
30. Wang, S.; Zhou, M.; Adhikari, K.; Zhuang, Q.; Bian, Z.; Wang, Y.; Jin, X. Anthropogenic Controls over Soil Organic Carbon Distribution from the Cultivated Lands in Northeast China. *Catena* **2022**, *210*, 105897. [\[CrossRef\]](#)
31. Minasny, B.; McBratney, A.B. Limited Effect of Organic Matter on Soil Available Water Capacity. *Eur. J. Soil Sci.* **2018**, *69*, 39–47. [\[CrossRef\]](#)
32. Fraterrigo, J.M.; Turner, M.G.; Pearson, S.M.; Dixon, P. Effects of Past Land Use on Spatial Heterogeneity of Soil Nutrients in Southern Appalachian Forests. *Ecol. Monogr.* **2005**, *75*, 215–230. [\[CrossRef\]](#)
33. Smith, P. Soil Organic Carbon Dynamics and Land-Use Change. In *Land Use and Soil Resources*; Springer: Dordrecht, The Netherlands, 2008; pp. 9–22. [\[CrossRef\]](#)
34. Bae, J.; Ryu, Y. Land Use and Land Cover Changes Explain Spatial and Temporal Variations of the Soil Organic Carbon Stocks in a Constructed Urban Park. *Landsc. Urban Plan.* **2015**, *136*, 57–67. [\[CrossRef\]](#)
35. Guo, L.B.; Gifford, R.M. Soil Carbon Stocks and Land Use Change: A Meta Analysis. *Glob. Chang. Biol.* **2002**, *8*, 345–360. [\[CrossRef\]](#)
36. Deng, L.; Zhu, G.; Tang, Z.; Shangguan, Z. Global Patterns of the Effects of Land-Use Changes on Soil Carbon Stocks. *Glob. Ecol. Conserv.* **2016**, *5*, 127–138. [\[CrossRef\]](#)
37. Guillaume, T.; Bragazza, L.; Levasseur, C.; Libohova, Z.; Sinaj, S. Long-Term Soil Organic Carbon Dynamics in Temperate Cropland-Grassland Systems. *Agric. Ecosyst. Environ.* **2021**, *305*, 107184. [\[CrossRef\]](#)
38. Pouyat, R.V.; Yesilonis, I.D.; Golubiewski, N.E. A Comparison of Soil Organic Carbon Stocks between Residential Turf Grass and Native Soil. *Urban Ecosyst.* **2008**, *12*, 45–62. [\[CrossRef\]](#)
39. Howard, D.M.; Howard, P.J.A.; Howard, D.C. A Markov Model Projection of Soil Organic Carbon Stores Following Land Use Changes. *J. Environ. Manag.* **1995**, *45*, 287–302. [\[CrossRef\]](#)
40. Kaye, J.P.; McCulley, R.L.; Burke, I.C. Carbon Fluxes, Nitrogen Cycling, and Soil Microbial Communities in Adjacent Urban, Native and Agricultural Ecosystems. *Glob. Chang. Biol.* **2005**, *11*, 575–587. [\[CrossRef\]](#)

41. Kaye, J.P.; Groffman, P.M.; Grimm, N.B.; Baker, L.A.; Pouyat, R. A Distinct Urban Biogeochemistry? *Trends Ecol. Evol.* **2006**, *21*, 192–199. [[CrossRef](#)] [[PubMed](#)]
42. Batjes, N.H. Total Carbon and Nitrogen in the Soils of the World. *Eur. J. Soil Sci.* **1996**, *47*, 151–163. [[CrossRef](#)]
43. Adhikari, K.; Hartemink, A.E.; Minasny, B.; Bou Kheir, R.; Greve, M.B.; Greve, M.H. Digital Mapping of Soil Organic Carbon Contents and Stocks in Denmark. *PLoS ONE* **2014**, *9*, e105519. [[CrossRef](#)]
44. Garten, C.T.; Ashwood, T.L. Landscape Level Differences in Soil Carbon and Nitrogen: Implications for Soil Carbon Sequestration. *Glob. Biogeochem. Cycles* **2002**, *16*, 61–1–61–14. [[CrossRef](#)]
45. Jackson, R.B.; Lajtha, K.; Crow, S.E.; Hugelius, G.; Kramer, M.G.; Piñeiro, G. The Ecology of Soil Carbon: Pools, Vulnerabilities, and Biotic and Abiotic Controls. *Annu. Rev. Ecol. Evol. Syst.* **2017**, *48*, 419–445. [[CrossRef](#)]
46. Viaud, V.; Angers, D.A.; Walter, C. Toward Landscape-Scale Modeling of Soil Organic Matter Dynamics in Agroecosystems. *Soil Sci. Soc. Am. J.* **2010**, *74*, 1847–1860. [[CrossRef](#)]
47. Hishi, T.; Hirobe, M.; Tateno, R.; Takeda, H. Spatial and Temporal Patterns of Water-Extractable Organic Carbon (WEOC) of Surface Mineral Soil in a Cool Temperate Forest Ecosystem. *Soil Biol. Biochem.* **2004**, *36*, 1731–1737. [[CrossRef](#)]
48. McBratney, A.B.; Mendonça Santos, M.L.; Minasny, B. On Digital Soil Mapping. *Geoderma* **2003**, *117*, 3–52. [[CrossRef](#)]
49. Breiman, L. Random Forests. *Mach. Learn.* **2001**, *45*, 5–32. [[CrossRef](#)]
50. Hengl, T.; de Jesus, J.M.; Heuvelink, G.B.M.; Gonzalez, M.R.; Kilibarda, M.; Blagotić, A.; Shangguan, W.; Wright, M.N.; Geng, X.; Bauer-Marschallinger, B.; et al. SoilGrids250m: Global Gridded Soil Information Based on Machine Learning. *PLoS ONE* **2017**, *12*, e0169748. [[CrossRef](#)]
51. Minasny, B.; McBratney, A.B. Digital Soil Mapping: A Brief History and Some Lessons. *Geoderma* **2016**, *264*, 301–311. [[CrossRef](#)]
52. Chen, S.; Martin, M.P.; Saby, N.P.A.; Walter, C.; Angers, D.A.; Arrouays, D. Fine Resolution Map of Top- and Subsoil Carbon Sequestration Potential in France. *Sci. Total Environ.* **2018**, *630*, 389–400. [[CrossRef](#)]
53. Mulder, V.L.; Lacoste, M.; Richer-de-Forges, A.C.; Arrouays, D. GlobalSoilMap France: High-Resolution Spatial Modelling the Soils of France up to Two Meter Depth. *Sci. Total Environ.* **2016**, *573*, 1352–1369. [[CrossRef](#)]
54. Arrouays, D.; Leenaars, J.G.B.; Richer-de-Forges, A.C.; Adhikari, K.; Ballabio, C.; Greve, M.; Grundy, M.; Guerrero, E.; Hempel, J.; Hengl, T.; et al. Soil Legacy Data Rescue via GlobalSoilMap and Other International and National Initiatives. *GeoResJ* **2017**, *14*, 1–19. [[CrossRef](#)]
55. Rossiter, D.G.; Poggio, L.; Beaudette, D.; Libohova, Z. How Well Does Predictive Soil Mapping Represent Soil Geography? An Investigation from the USA. *Soil Discuss.* **2021**, 1–35. [[CrossRef](#)]
56. Libohova, Z.; Wills, S.; Odgers, N.P. Legacy Data Quality and Uncertainty Estimation for United States GlobalSoilMap Products. In *GlobalSoilMap: Basis of the Global Spatial Soil Information System, Proceedings of the 1st GlobalSoilMap Conference, Orléans, France, 7–9 October 2013*; CRC Press: Boca Raton, FL, USA, 2014; pp. 63–68. [[CrossRef](#)]
57. Minasny, B.; Sulaeman, Y.; Mcbratney, A.B. Is Soil Carbon Disappearing? The Dynamics of Soil Organic Carbon in Java. *Glob. Chang. Biol.* **2011**, *17*, 1917–1924. [[CrossRef](#)]
58. Soil Survey Staff. Gridded Soil Survey Geographic (gSSURGO) Database for North Carolina. United States Department of Agriculture, Natural Resources Conservation Service. Available online: <https://gdg.sc.egov.usda.gov/> (accessed on 30 May 2020).
59. Soil Survey Staff, Natural Resources Conservation Service, United States Department of Agriculture. Official Soil Series Descriptions. Available online: <https://www.nrcs.usda.gov/wps/portal/nrcs/main/soils/survey/> (accessed on 30 May 2022).
60. FAO. *Measuring and Modelling Soil Carbon Stocks and Stock Changes in Livestock Production Systems: Guidelines for Assessment*; FAO: Rome, Italy, 2019; p. 170.
61. Minasny, B.; McBratney, A.B. A Conditioned Latin Hypercube Method for Sampling in the Presence of Ancillary Information. *Comput. Geosci.* **2006**, *32*, 1378–1388. [[CrossRef](#)]
62. Wilson, J.; Gallant, J. *Terrain Analysis: Principles and Applications*; Wiley: New York, NY, USA, 2000; pp. 51–85.
63. Beven, K.J.; Kirkby, M.J. A Physically Based, Variable Contributing Area Model of Basin Hydrology. *Hydrol. Sci. Bull.* **1979**, *24*, 43–69. [[CrossRef](#)]
64. MacMillan, R.A.; Pettapiece, W.W.; Nolan, S.C.; Goddard, T.W. A Generic Procedure for Automatically Segmenting Landforms into Landform Elements Using DEMs, Heuristic Rules and Fuzzy Logic. *Fuzzy Sets Syst.* **2000**, *113*, 81–109. [[CrossRef](#)]
65. Schoeneberger, P.; Wysocki, D.; Benham, E. *Soil Survey Staff Field Book for Describing and Sampling Soils*, 3rd ed.; National Soil Survey Center, National Resources Conservation Service: Lincoln, NE, USA, 2012.
66. Burt, R. *Soil Survey Staff Kellogg Soil Survey Laboratory Methods Manual*; Soil Survey Investigations Report No. 42, Version 5.0; Natural Resources Conservation Service Soils: Washington, DC, USA, 2014.
67. California Carbon Allowance (CCA) Program. Available online: <https://www.californiacarbon.info> (accessed on 6 January 2022).
68. Odeh, I.O.A.; McBratney, A.B.; Chittleborough, D.J. Further Results on Prediction of Soil Properties from Terrain Attributes: Heterotopic Cokriging and Regression-Kriging. *Geoderma* **1995**, *67*, 215–226. [[CrossRef](#)]
69. Hengl, T.; Heuvelink, G.B.M.; Stein, A. A Generic Framework for Spatial Prediction of Soil Variables Based on Regression-Kriging. *Geoderma* **2004**, *120*, 75–93. [[CrossRef](#)]
70. R Studio Team. *R Studio*; R Studio Team: Boston, MA, USA, 2021.
71. Guo, Z.; Adhikari, K.; Chellasamy, M.; Greve, M.B.; Owens, P.R.; Greve, M.H. Selection of Terrain Attributes and Its Scale Dependency on Soil Organic Carbon Prediction. *Geoderma* **2019**, *340*, 303–312. [[CrossRef](#)]
72. Minasny, B.; McBratney, A.B.; Malone, B.P.; Wheeler, I. Digital Mapping of Soil Carbon. *Adv. Agron.* **2013**, *118*, 1–47. [[CrossRef](#)]

73. Cambardella, C.A.; Moorman, T.B.; Novak, J.M.; Parkin, T.B.; Karlen, D.L.; Turco, R.F.; Konopka, A.E. Field-Scale Variability of Soil Properties in Central Iowa Soils. *Soil Sci. Soc. Am. J.* **1994**, *58*, 1501–1511. [\[CrossRef\]](#)
74. Adhikari, K.; Mishra, U.; Owens, P.R.; Libohova, Z.; Wills, S.A.; Riley, W.J.; Hoffman, F.M.; Smith, D.R. Importance and Strength of Environmental Controllers of Soil Organic Carbon Changes with Scale. *Geoderma* **2020**, *375*, 114472. [\[CrossRef\]](#)
75. Ramcharan, A.; Hengl, T.; Nauman, T.; Brungard, C.; Waltman, S.; Wills, S.; Thompson, J. Soil Property and Class Maps of the Conterminous United States at 100-Meter Spatial Resolution. *Soil Sci. Soc. Am. J.* **2018**, *82*, 186–201. [\[CrossRef\]](#)
76. Seybold, C.A.; Ferguson, R.; Wysocki, D.; Bailey, S.; Anderson, J.; Nester, B.; Schoeneberger, P.; Wills, S.; Libohova, Z.; Hoover, D.; et al. Application of Mid-Infrared Spectroscopy in Soil Survey. *Soil Sci. Soc. Am. J.* **2019**, *83*, 1746–1759. [\[CrossRef\]](#)
77. Poeplau, C.; Don, A. Sensitivity of Soil Organic Carbon Stocks and Fractions to Different Land-Use Changes across Europe. *Geoderma* **2013**, *192*, 189–201. [\[CrossRef\]](#)
78. Martin, M.P.; Wattenbach, M.; Smith, P.; Meersmans, J.; Jolivet, C.; Boulonne, L.; Arrouays, D. Spatial Distribution of Soil Organic Carbon Stocks in France. *Biogeosciences* **2011**, *8*, 1053–1065. [\[CrossRef\]](#)
79. Wiesmeier, M.; Barthold, F.; Blank, B.; Kögel-Knabner, I. Digital Mapping of Soil Organic Matter Stocks Using Random Forest Modeling in a Semi-Arid Steppe Ecosystem. *Plant Soil* **2011**, *340*, 7–24. [\[CrossRef\]](#)
80. Davis, J.E.; Mcrae, C.; Estep, B.L.; Barden, L.S.; Matthews, J.F. Vascular Flora of Piedmont Prairies: Evidence from Several Prairie Remnants. *Castanea* **2002**, *67*, 1–12.
81. Hurriss, T.T.; Norton, J.B.; Norton, U. Soil Profile Carbon and Nitrogen in Prairie, Perennial Grass–Legume Mixture and Wheat-Fallow Production in the Central High Plains, USA. *Agric. Ecosyst. Environ.* **2013**, *181*, 179–187. [\[CrossRef\]](#)
82. Libbey, K.; Hernández, D.L. Depth Profile of Soil Carbon and Nitrogen Accumulation over Two Decades in a Prairie Restoration Experiment. *Ecosystems* **2021**, *24*, 1348–1360. [\[CrossRef\]](#)
83. Vicente, L.C.; Gama-Rodrigues, E.F.; Gama-Rodrigues, A.C. Soil Carbon Stocks of Ultisols under Different Land Use in the Atlantic Rainforest Zone of Brazil. *Geoderma Reg.* **2016**, *7*, 330–337. [\[CrossRef\]](#)
84. Nwaogu, C.; Okeke, O.J.; Fashae, O.; Nwankwoala, H. Soil Organic Carbon and Total Nitrogen Stocks as Affected by Different Land Use in an Ultisol in Imo Watershed, Southern Nigeria. *Chem. Ecol.* **2018**, *34*, 854–870. [\[CrossRef\]](#)
85. O'Rourke, S.M.; Angers, D.A.; Holden, N.M.; McBratney, A.B. Soil Organic Carbon across Scales. *Glob. Chang. Biol.* **2015**, *21*, 3561–3574. [\[CrossRef\]](#)
86. Don, A.; Schumacher, J.; Scherer-Lorenzen, M.; Scholten, T.; Schulze, E.-D. Spatial and Vertical Variation of Soil Carbon at Two Grassland Sites—Implications for Measuring Soil Carbon Stocks. *Geoderma* **2007**, *141*, 272–282. [\[CrossRef\]](#)
87. Rodríguez Martín, J.A.; Álvaro-Fuentes, J.; Gonzalo, J.; Gil, C.; Ramos-Miras, J.J.; Grau Corbí, J.M.; Boluda, R. Assessment of the Soil Organic Carbon Stock in Spain. *Geoderma* **2016**, *264*, 117–125. [\[CrossRef\]](#)
88. Shrestha, B.M.; Sitaula, B.K.; Singh, B.R.; Bajracharya, R.M. Soil Organic Carbon Stocks in Soil Aggregates under Different Land Use Systems in Nepal. *Nutr. Cycl. Agroecosyst.* **2004**, *70*, 201–213. [\[CrossRef\]](#)
89. Vanhala, P.; Karhu, K.; Tuomi, M.; Sonninen, E.; Jungner, H.; Fritze, H.; Liski, J. Old Soil Carbon Is More Temperature Sensitive than the Young in an Agricultural Field. *Soil Biol. Biochem.* **2007**, *39*, 2967–2970. [\[CrossRef\]](#)
90. Rosenbloom, N.A.; Harden, J.W.; Neff, J.C.; Schimel, D.S. Geomorphic Control of Landscape Carbon Accumulation. *J. Geophys. Res. Biogeosci.* **2006**, *111*, G01004. [\[CrossRef\]](#)
91. Singh, P.; Benbi, D.K. Soil Organic Carbon Pool Changes in Relation to Slope Position and Land-Use in Indian Lower Himalayas. *Catena* **2018**, *166*, 171–180. [\[CrossRef\]](#)
92. Mishra, U.; Lal, R.; Liu, D.; van Meirvenne, M. Predicting the Spatial Variation of the Soil Organic Carbon Pool at a Regional Scale. *Soil Sci. Soc. Am. J.* **2010**, *74*, 906–914. [\[CrossRef\]](#)
93. Chaney, N.W.; Minasny, B.; Herman, J.D.; Nauman, T.W.; Brungard, C.W.; Morgan, C.L.S.; McBratney, A.B.; Wood, E.F.; Yimam, Y. POLARIS Soil Properties: 30-m Probabilistic Maps of Soil Properties Over the Contiguous United States. *Water Resour. Res.* **2019**, *55*, 2916–2938. [\[CrossRef\]](#)
94. Grüneberg, E.; Schöning, I.; Kalko, E.K.V.; Weisser, W.W. Regional Organic Carbon Stock Variability: A Comparison between Depth Increments and Soil Horizons. *Geoderma* **2010**, *155*, 426–433. [\[CrossRef\]](#)
95. Finke, P.; Hartwich, R.; Dudal, R.; Ibañez, J.; Jamagne, M.; King, D.; Montanarella, L.; Yassoglou, N. *Georeferenced Soil Database for Europe: Manual of Procedures*; Version 1.1; Office for Official Publications of the European Communities: Luxembourg, 1998.
96. Grunwald, S.; Thompson, J.A.; Boettinger, J.L. Digital Soil Mapping and Modeling at Continental Scales: Finding Solutions for Global Issues. *Soil Sci. Soc. Am. J.* **2011**, *75*, 1201–1213. [\[CrossRef\]](#)
97. Minasny, B.; Malone, B.P.; McBratney, A.B. Digital Soil Assessments and beyond. In Proceedings of the 5th Global Workshop on Digital Soil Mapping, Sydney, Australia, 10–13 April 2012; CRC Press: Boca Raton, FL, USA, 2012. ISBN 9780415621557.
98. Pouyat, R.V.; Yesilonis, I.D.; Nowak, D.J. Carbon Storage by Urban Soils in the United States. *J. Environ. Qual.* **2006**, *35*, 1566–1575. [\[CrossRef\]](#) [\[PubMed\]](#)